THE LOW TEMPERATURE THERMAL CONDUCTIVITY OF CESIUM IODIDE

by

DAVID LAWRENCE JOHNSON
B.Sc., The University of British Columbia, 1963

A THESIS SUBMITTED IN PARTIAL FULFILMENT OF
THE REQUIREMENTS FOR THE DEGREE OF
MASTER OF SCIENCE

in the Department
of
Physics

We accept this thesis as conforming to the
required standard

THE UNIVERSITY OF BRITISH COLUMBIA
February, 1967

In presenting this thesis in partial fulfilment of the requirements for an advanced degree at the University of British Columbia, I agree that the Library shall make it freely available for reference and study. I further agree that permission for extensive copying of this thesis for scholarly purposes may be granted by the Head of my Department or by his representatives. It is understood that copying or publication of this thesis for financial gain shall not be allowed without my written permission.

Department of PHYSICS

The University of British Columbia
Vancouver 8, Canada

Date MARCH 20, 1967.

ABSTRACT

The thermal conductivity of three crystals of cesium iodide ranging in size from three to eight millimeters diameter was measured in the temperature range 1.15°K to 5.40°K.

Thermal conductivity measurements were made using the thermal potentiometer method.

Differences in the thermal conductivity of the three samples were interpreted in terms of phonon scattering from the boundaries of the crystals, and from internal structure defects.

DEDICATED

to my father

FRANCIS HENRY JOHNSON

who is a humanist

but will enjoy it regardless.

TABLE OF CONTENTS

LIST OF TABLES

LIST OF FIGURES

Acknowledgements

I would like to thank Dr. M.J. Crooks for his original suggestion of this research project, and for his thoughtful supervision of my work.

I am indebted also to Mr. R. Weisbach and Mr. G. Brooks for their technical assistance, and to Dr. P.R. Critchlow and Mr. C.R. Brown for discussion of the theoretical questions.

Particular thanks are due to my mother, Mrs. F.H. Johnson for the excellence of her typing, and to my wife Elizabeth for her help and patience.

CHAPTER I. THEORY

(1) INTRODUCTION

The successful liquefaction of helium in 1908 made possible the combined theoretical and experimental investigation of heat transfer at low temperatures. It was quickly realized that the mechanisms of heat transfer in a metal would be at least partially different from those in a non-metal.

The groundwork for the current theory of heat transfer in dielectric crystals was laid by Peierls, with his quantum mechanical analysis of the interaction of lattice waves in a crystal. (Peierls 1929)

(a) Crystal Lattice Vibrations. In a dielectric crystal the atoms of the crystal are vibrating, and these vibrations are linked or coupled by the interatomic forces in the crystal. The total thermal energy of the crystal is thought to be contained in all the possible normal modes of vibration of the crystal lattice.

If we neglect the zero point energy, then for a dielectric crystal at temperature T°K, the average energy in a vibration mode of frequency ν is

$$\frac{h\nu}{\exp(h\nu/KT) - 1}$$

This energy may be considered as being made up of $1/[\exp(h\nu/KT) - 1]$ quanta of vibrational energy, each with energy $h\nu$. These quanta of vibrational energy have come to be called phonons, and their distribution with respect to the frequency ν is called the phonon spectrum of the material at temperature T°K.

One can easily slip into a billiard ball concept of phonons, as one can with photons, but in both cases care must be exercised in the application of this concept.

(b) Heat Flow. Consider groups of phonons with angular frequencies near $\omega(=2\pi\nu)$ and wave numbers near $\vec{q}$. The group velocities $\vec{v}(\vec{q})$ of these packets will be given by $d\omega/dq$. If the phonon spectrum of the material is such that there are a number $N(q)$ phonons in mode q, the heat current will be

$$\vec{Q} = \sum N(\vec{q})\hbar\omega\vec{v}(\vec{q}) \qquad (1)$$

In thermal equilibrium, the net flow of phonons in any direction is zero, or $N_o(\vec{q}) = N_o(-\vec{q})$.

However, if a temperature gradient exists, there will be a density gradient in the phonons, resulting in a net flow. This tends to alter the phonon population at a given point from $N_o(q)$ to $N(q)$.

When the situation is reached whereby this tendency to alter $N_o(q)$ is balanced by the tendency of scattering processes to restore the equilibrium population $N_o(q)$, a steady

state condition is attained with a finite heat flow $\vec{Q}$ and a finite temperature gradient $\vec{\nabla}T$.

The magnitude of the heat flow, and hence of the thermal conductivity, is determined by the amount of departure of $N(q)$ from $N_o(q)$.

(c) Boltzmann Equation. The condition whereby the drift of phonons due to a temperature gradient is balanced by the processes which scatter them is expressed in the Boltzmann equation.

$$\left[\frac{\partial N(q)}{\partial t}\right]_{DRIFT} + \left[\frac{\partial N(q)}{\partial t}\right]_{SCATTER} = 0 \qquad \text{-------(2)}$$

A complete solution of this equation, and the resulting calculation of the phonon spectrum, would result in complete predictability of the thermal conductivity of a dielectric material. In general this equation cannot be solved explicitly, and various approximations must be used. The approximation which has found most application is the

(d) Additive Relaxation Rate Approximation. In the relaxation time method of solution of (2) it is assumed that the return of a phonon distribution $N(q)$ to its equilibrium distribution $N_o(q)$ is exponential with time. This can be expressed as

$$\left[\frac{\partial N(q)}{\partial t}\right]_{SCATTER} = \frac{N_o(q) - N(q)}{\tau(q)} \qquad \text{---------(3)}$$

where $1/\tau(q)$ is termed the relaxation rate.

In any real crystal, there may be several processes

tending to restore the equilibrium phonon distribution, each with its own relaxation rate. If these processes are mutually non-interfering, then we would expect their relaxation rates to be additive,

$$\frac{1}{\tau(q)} = \frac{1}{\tau_1(q)} + \frac{1}{\tau_2(q)} + \frac{1}{\tau_3(q)} + \cdots\cdots \quad (4)$$

Scattering processes which are considered to be non-interfering are (Carruthers, 1961);

- τ_b boundary scattering,
- τ_I isotope (mass-difference) scattering,
- τ_p point defect scattering,
- τ_D dislocation scattering,
- τ_U Umklapp or U-processes, and
- τ_N normal or N-process.

(e) Normal and Umklapp Processes. In all real crystals, the interatomic forces are anharmonic. This leads to an interaction between phonons in the body of an otherwise "perfect" and infinite crystal. At low temperatures interactions or "collisions" involving three phonons are the most important. The first anharmonic term in an expansion of the interatomic force is the cubic term, and this term leads to three phonon interactions.

In phonon collisions such as these, energy is conserved, while phonon wave number may be either conserved or altered

by a reciprocal lattice vector $\vec{b}$. Note that the number of phonons is not conserved. We may then write the conservation relations,

$$\hbar\omega_1 + \hbar\omega_2 = \hbar\omega_3, \quad \text{(5a)},$$

$$\vec{q}_1 + \vec{q}_2 = \vec{q}_3 + \vec{b}, \quad \text{(5b)},$$

$$\vec{q}_1 + \vec{q}_2 = \vec{q}_3. \quad \text{(5c)}.$$

If $\vec{b}$ is a reciprocal lattice vector (5b) the collision is called an Umklapp or U-process, while if b = 0 (5c) the collision is called a Normal or N-process.

(f) Solution via Relaxation Time Approximation. If we consider a material which exhibits no scattering mechanisms other than those of sec. (e) above, then we may use the relaxation time approximation (3) to solve the Boltzmann equation (2). Doing so leads (Berman, 1965; Callaway, 1959) to a thermal conductivity given by

$$k = \frac{1}{3}\int C(q)\, v^2(q)\tau(q)dq \quad \text{(6)}$$

where C(q) is the contribution to the specific heat from phonon packets of wave number q.

(g) Debye Solid Assumption. Let us now suppose that the phonon group velocity is a constant c independent of the phonon wave number q. This is referred to as the Debye approximation

$$\omega(q) = cq.$$

A "Debye solid" is a model in which there is a constant

phonon velocity c and a characteristic temperature θ_D.

Using this model, one can derive (Makinson, 1938; Callaway, 1959) a thermal conductivity given by

$$k = \frac{K^4}{2\pi^2\hbar^3} \cdot \langle c^{-1} \rangle \cdot T^3 \int_0^{\theta_D/T} \tau_R \frac{x^4 e^x}{(e^x-1)^2} \, dx \quad \text{------ (7)},$$

where K is Boltzmann's constant, $\hbar$ is Planck's constant, $x = \hbar\omega/KT$, τ_R is a relaxation time and $\langle c^{-1} \rangle$ is some average value of the inverse velocities of sound over all directions and polarizations in a crystal. This expression will be referred to as the Debye approximation to Callaway's theory.

(h) Temperature Variation of Thermal Conductivity. With reference to (6), we may now define three distinct types of temperature variation in the thermal conductivity.

(i) I/T region. At high temperatures the main scattering mechanism is phonon-phonon collision. If the temperature is high enough, say greater than θ_D, then the dominant phonon wave numbers are sufficiently great so that a large fraction of all phonons are available for combinations of the type (5b). Umklapp interactions are then the major scattering process. The relaxation rate τ_R^{-1} is proportional to the phonon density and hence to absolute temperature, (since phonons obey Bose-Einstein statistics). The dominant phonon modes make a constant contribution to the specific heat and hence by (6) we obtain $k \propto I/T$.

(ii) Exponential region. As the temperature decreases, the specific heat term in (6) decreases, but the number of phonons available to participate in U-processes decreases exponentially. The scattering time thus increases so rapidly with temperature drop as to be nearly exponential, and by (6) the thermal conductivity is therefore $k \propto \exp(a/T)$.

(iii) Boundary scattering region. At very low temperatures the scattering time τ will increase to the point where it is comparable with the time taken for phonons to cross the entire crystal without scattering. When this occurs, the major scattering mechanism is the boundaries of the sample. We may then write, if c is the phonon velocity and D is the diameter of the crystal, $\tau \cong D/c$. At these temperatures the specific heat is usually well into the T^3 region, and by (6) we may therefore write

$$k \propto DT^3 \qquad \text{(8)}.$$

(2) SIZE DEPENDENT THERMAL CONDUCTIVITY.

(a) Theoretical Work. The first satisfactory theoretical explanation of size dependent thermal conductivity was Casimir's attempt (Casimir 1938) to explain the experimental results of de Haas and Biermasz (de Haas and Biermasz, 1938). Casimir applies the standard blackbody radiation theory to a phonon gas. He considers a long cylindrical tube of diameter D, with perfectly black walls (i.e. all phonon reflections

are diffuse) at a temperature low enough that the only phonon scattering mechanism is the boundaries of the crystal.

Casimir obtains the result (after making a correction of $2/\pi$ as noted in [Berman et al, 1953]),

$$k = \frac{2\pi^2 K^4}{15\hbar^3}\left[\frac{1}{3}\left(\sum\frac{1}{v_i^2}\right)\right] DT^3 \quad \text{---------- (9)}$$

where the term in square brackets is an attempt to find a value for the average velocity of sound over all polarizations and all directions in the crystal. If we replace this with the notation $\langle c^{-2}\rangle$, we obtain

$$k = \frac{2\pi^2 K^4}{15\hbar^3}\langle c^{-2}\rangle DT^3 \quad \text{---------- (10)},$$

in agreement with (8).

Casimir also obtained the relation between thermal conductivity and specific heat

$$k = 1.155 \times 10^3 A^{2/3} P D T^3 \quad \text{---------- (11)},$$

where A is the constant in the specific heat equation $C_v = AT^3$ Joule/cm^3 °K, and

$$P = \frac{\langle c^{-2}\rangle}{\langle c^{-3}\rangle^{2/3}} \quad \text{---------- (12)}.$$

(b) Previous Experimental Work. Numerous experimenters have tried to match observed boundary scattering behaviour with theory. Measurements on an artificial sapphire crystal (Berman et al, 1955) showed a thermal conductivity which was

directly proportional to crystal diameter, but agreement with the theoretical magnitude of the conductivity was obtained only after making corrections for the finite length of the sample, and for a presumed partially specular phonon reflection from the boundaries.

The best experimental agreement with Casimir's theory was obtained by Thatcher (Thatcher, 1965) using crystals of LiF. Calculation of k for LiF via the Casimir theory leads to the result

$$k = 0.172\ DT^3 \text{ watt/cm}^\circ\text{K} \quad \text{---------- (13)} .$$

Thatcher obtained the result

$$k = (0.21 \pm 0.02)DT^n, \quad \text{---------- (14)}$$
$$n = 3.005 \pm 0.015.$$

The 20% deviation in magnitude from the calculated value was presumed to be due to an inability to correctly calculate the average sound velocities in an anisotropic crystal.

(3) CHOICE OF CsI AS AN EXPERIMENTAL SUBSTANCE.

The "ideal" crystal for investigation of low temperature Thermal conductivity would be a single crystal of chemically and isotopically pure material, homogeneous and isotropic in its thermal properties, and easily handled.

Since a material was desired which, in some temperature range, exhibited phonon scattering by boundaries only, the

elimination of point defect scattering was necessary, that is the material was to be very pure. Alkali halides have attracted much interest as pseudo-Debye solids. Both cesium and iodine have only one naturally occurring stable isotope, and thus the isotopic purity of CsI is guaranteed.

Past experience with materials exhibiting the boundary scattering region has shown the thermal conductivity peak to lie at approximately 1/30 of the Debye temperature, θ_D. For CsI, θ_D is about 125°K, placing the expected peak at around 4.1°K and thus making the boundary scattering region easily accessible with a helium-4 cryostat.

CsI has also been suggested as a possible candidate in the search for second sound in solids (C.R. Brown, private communication). The ratio of atomic weights of Cs to I is only 1.05, closer to one than any other alkali halide. It has been suggested that this property would increase the probability of finding a Poiseuille flow "window" (Guyer et al, 1966) in the temperature wave frequency vs. temperature behaviour.

(4) CALCULATION OF k FOR CsI.

(a) Anisotropy. The major computational problem involved in a calculation of k for CsI is that of finding suitable average values for the velocities of sound in the crystal. CsI crystallizes in the CsCl structure and has therefore a

simple cubic structure with one molecule or two atoms /unit cell.

The anisotropy factor η of a material is given in terms of the elastic constants by

$$\eta = \frac{2c_{44}}{c_{11}-c_{12}} \quad \text{----------} \quad (15)$$

Using the elastic constants measured at low temperature (Vallin et al, 1964) we obtain for CsI

$$\eta = .85 \quad \text{----------} \quad (16).$$

The Houston approximation (Houston, 1948; Betts et al, 1956) is a method for finding the approximate value of an angular integral given the value of the integrand in three mutually perpendicular directions.

It is found (Betts et al, 1956) that for anisotropy factors in the range $.5<\eta<1.5$, Houston's approximation is not appreciably different from approximations involving more known directions, for the calculation of average velocities of sound.

(b) Velocities of Sound in the $\langle 100 \rangle$, $\langle 110 \rangle$, $\langle 111 \rangle$ Directions.

Given the three elastic constants c_{11}, c_{12}, c_{44}, and the density ρ, the seven "basic" velocities of sound are given by

A $\langle 100 \rangle$ $\quad v_{t_1}\langle 100\rangle = v_{t_2}\langle 100\rangle = \left(\frac{c_{44}}{\rho}\right)^{1/2}$

$$v_\ell \langle 100\rangle = \left(\frac{c_{11}}{\rho}\right)^{1/2}$$

B $\langle 110 \rangle$ $\quad v_{t_1}\langle 110\rangle = \left(\frac{c_{44}}{\rho}\right)^{1/2}$

$$v_{t_2}\langle 110\rangle = \left(\frac{c_{11} - c_{12}}{2\rho}\right)^{1/2}$$

$$v_\ell\langle 110\rangle = \left(\frac{c_{44} + 1/2(c_{11} + c_{12})}{\rho}\right)^{1/2}$$

C $\langle 111 \rangle$ $\quad v_{t_1}\langle 111\rangle = v_{t_2}\langle 111\rangle = \left(\frac{c_{44} + c_{11} - c_{12}}{3\rho}\right)^{1/2}$

$$v_\ell \langle 111\rangle = \left(\frac{4c_{44} + 2c_{12} + c_{11}}{3\rho}\right)^{1/2}.$$

Using the density and elastic constants measured by Vallin, we obtain for CsI the results shown in Table I.

(c) Average Velocities of Sound.

(i) Suppose it is desired to find J, the angular integral of some integrand $I(\theta,\varphi)$,

$$J = \int I(\theta,\varphi)\, d\Omega,$$

then Houston's method states that if I_a, I_b, and I_c are the known values of the integrand in the directions $\langle 100\rangle$, $\langle 110\rangle$, and $\langle 111\rangle$ respectively, then we can approximate the integral by

$$J = \int I(\theta,\varphi)\, d\Omega$$

$$\cong \frac{4\pi}{35}\left(10I_a + 16I_b + 9I_c\right) \text{---------- (17).}$$

(ii) We wish to find the three averages over direction and polarizations,

$$\langle c^{-n} \rangle = \int \frac{I_n(\theta,\varphi)\, d\Omega}{12\pi} \qquad \text{----------(18)},$$

where $I_n = \sum_{i=1}^{3} \left\{ \frac{1}{v_i^n} \right\}$, n = (1, 2, 3).
The sum over i = (1, 2, 3) represents the sum of the three different polarizations, two transverse and one longitudinal. The factor of 12π is a normalization factor equal to 3 x 4π, 3 from the three polarizations and 4π from the total solid angle.

The results of this calculation are shown in Table I.

(d) Conductivity Calculations. Using the results obtained in the previous section, we may now calculate the theoretical thermal conductivity of CsI in the boundary scattering region.

At temperatures sufficiently low that phonons are scattered only at the boundaries of the crystal the relaxation time τ_R in equation (7) becomes a constant τ_b, and $\theta_D/T \longrightarrow \infty$ whence the integral in (7) may be set equal to 26.0. We thus obtain

$$k = \frac{26.0\, K^4}{2\pi^2 \hbar^3} \langle c^{-1} \rangle \tau_b T^3 ,$$

TABLE I

Average and Particular Sound Velocities in CsI

Direction	Polarization	Velocity
$\langle 100 \rangle$	t	1.323×10^5 cm/sec
	l	2.410
$\langle 110 \rangle$	t	1.323
	t	1.436
	l	2.345
$\langle 111 \rangle$	t	1.400
	l	2.322

$$\langle c^{-1} \rangle = .629 \times 10^{-5} = (1.59 \times 10^5)^{-1} \text{ (cm/sec)}^{-1}$$

$$\langle c^{-2} \rangle = .417 \times 10^{-10} = (1.55 \times 10^5)^{-2} \text{ (cm/sec)}^{-2}$$

$$\langle c^{-3} \rangle = .287 \times 10^{-15} = (1.52 \times 10^5)^{-3} \text{ (cm/sec)}^{-3}$$

Based on 4.2°K values (Vallin et al, 1964) of

$$\rho = 4.712 \text{ gm/cm}^3$$
$$c_{11} = 2.737 \times 10^{11} \text{ dynes/cm}^2$$
$$c_{12} = .793 \quad " \quad "$$
$$c_{44} = .825 \quad " \quad "$$

and substituting for the constants and the calculated value of $\langle c^{-1} \rangle$ we obtain

$$k = 2.57 \times 10^{5} \tau_b T^3 \text{ ---------- (19).}$$

We now take τ_b to be the "time of flight" across a diameter of the crystal,

$$\tau_b = D\langle c^{-1} \rangle = .629 \times 10^{-5} D \text{ sec ---------- (20),}$$

and by substitution into (19) we obtain

$$k = 1.62\ DT^3 \text{ watt/cm°K ---------- (21).}$$

Working directly from the Casimir equation (10), and substituting for the constants and $\langle c^{-2} \rangle$ we obtain

$$k = 1.70\ DT^3 \text{ watt/cm°K ---------- (22).}$$

We may also work from Casimir's specific heat equation (11). The specific heat of CsI has been measured (Taylor et al, 1962) down to 13.51°K, at which temperature it was found to be $C_p = 1.927$ cal/mole°K. A simple calculation shows that

$$C_p - C_v \cong .001 \text{ cal/mole°K ----------,}$$

hence $C_v = 1.926$ cal/mole°K at 13.51°K. If we assume that at this temperature

$$C_v = AT^3 \text{ ---------- ,}$$

we find

$$A = 57.17 \times 10^{-6} \text{ watt-sec/cm}^3\text{°K}^4 \text{ ---------- ,}$$

and

$$A^{2/3} = 1.484 \times 10^{-3} (\text{watt-sec/cm}^3\text{°K}^4)^{2/3} \text{ --------- (23).}$$

Substituting values of $\langle c^{-2} \rangle$ and $\langle c^{-3} \rangle$ we obtain

$$P = \frac{\langle c^{-2} \rangle}{\langle c^{-3} \rangle^{2/3}} = .96 \text{ ---------- (24),}$$

Casimir's specific heat equation then leads to the result

$$k = 1.64 \, DT^3 \text{ ---------- (25).}$$

Comparing the three theoretical results, we may then say that theory predicts for CsI a thermal conductivity in the boundary scattering region which is proportional to the sample diameter D, the cube of the absolute temperature, and is of magnitude

$$k \cong 1.65 \, DT^3 \text{ watt/cm°K ---------- (26).}$$

(5) EXPERIMENT.

The experiment used rods of CsI of varying diameters D. The temperature difference $\triangle T$ between two thermometers a distance L apart was measured during the passage of a known

heat current P through the sample. The thermal conductivity was then taken to be

$$k = \frac{P}{\Delta T} \cdot \frac{L}{A}$$

$$= \frac{P}{\Delta T} \cdot \frac{4L}{\pi D^2} \quad \text{---------- (27).}$$

All quantities on the right of equation (27) may be measured, whence the thermal conductivity of the sample may be found.

CHAPTER II. APPARATUS.

(1) THERMAL

(a) Low Temperature Production. The experiment was carried out in a liquid helium-4 cryostat capable of reaching and controlling temperatures from 4.29°K to 1.12°K. Both the inner liquid helium dewar and the outer liquid nitrogen dewar were of Pyrex glass, silvered except for vertical slits down both sides and sealed under vacuum. Liquid level was observed using a fluorescent tube parallel to one set of slits.

The top of the helium dewar consisted of 18cm. of single thickness Pyrex pipe, so that the double walled section of the helium dewar could be kept entirely below the liquid nitrogen level. Care was taken never to admit helium gas or liquid into the helium dewar unless it was cooled to nitrogen temperature. With this procedure, diffusion of helium through the helium dewar walls was kept to a minimum. It was found that a dewar lasted for about twenty runs, or roughly two hundred hours, before it was necessary to break it open and re-evacuate the interspace.

Both dewars were supported from the end of a 4" pumping line capped with a 3" Grinnell-Saunders rubber diaphragm valve. (Fig. 1, #7) Pumping of the helium bath was done by a Stokes Microvac Model 49-10 Rotary vacuum pump with a capacity of 80 cubic feet per minute.

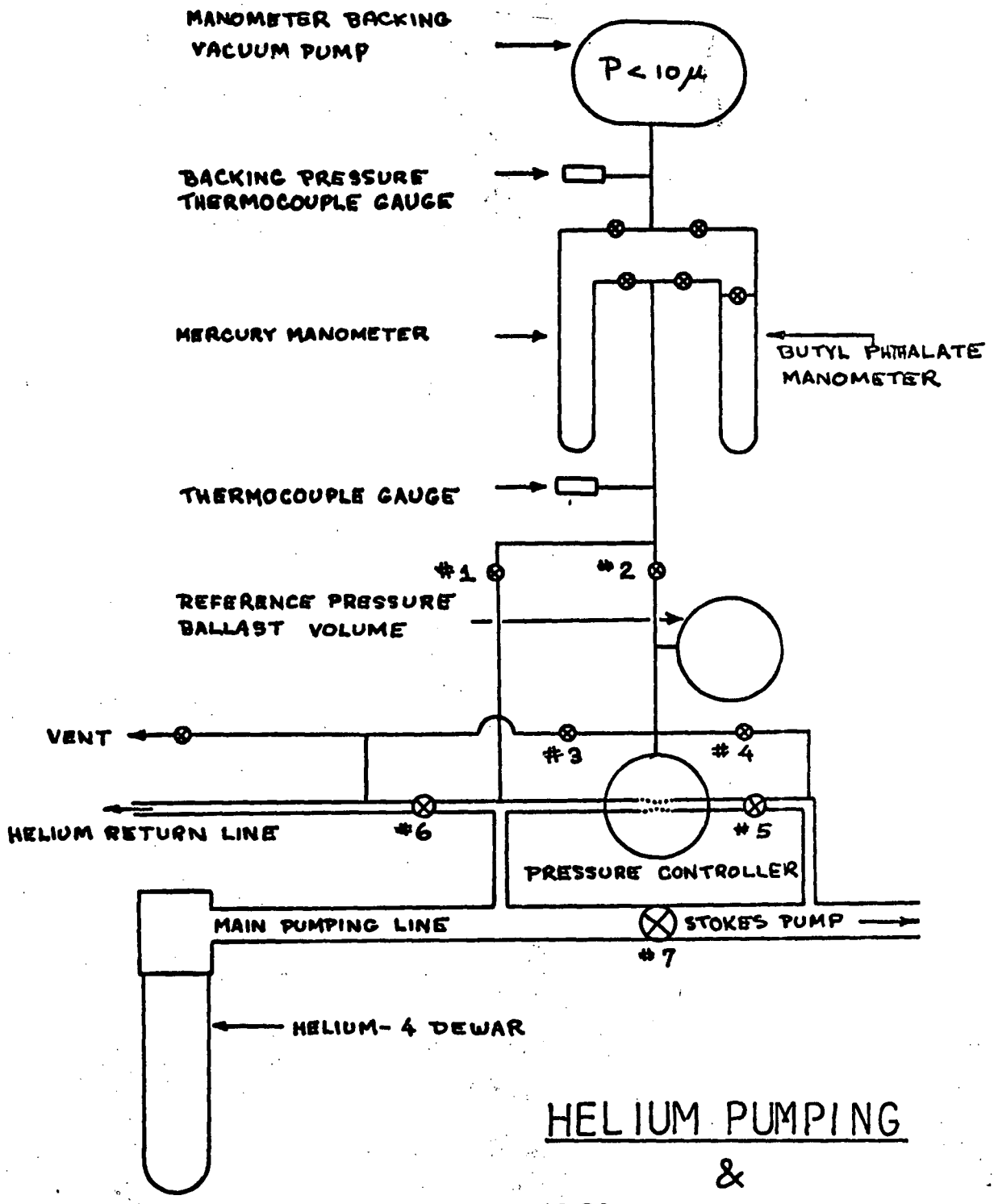

HELIUM PUMPING & CONTROL SYSTEM

FIGURE 1

(b) Temperature Control. Due to the long thermal equilibrium times encountered, (up to 40 min.), a stable method of temperature control was necessary. A modified version of the apparatus of Walker (1959) was adopted. It consisted, essentially, of a 1" pumping line in parallel with the 3" diaphragm value. A short section of the pumping line was replaced by a piece of thin walled (.002") rubber tubing, (nominally sold only for the prevention of disease), which acted as a valve controlled by the reference pressure in a closed volume of gas surrounding it. Connection of the reference volume (10 liters) to manometers, (Fig. 1, valve #2) vacuum line, (Fig. 1, valve #4) and helium gas line, (Fig. 1, valve #3) facilitated quick and easy selection of any desired bath temperature.

This device maintained pressures from .500mmHg to 800mmHg stable to better than 50μ over periods of three or four hours. The major cause of drift was slow changes of room temperature resulting in slight changes of the gas pressure in the reference volume. Diffusion of helium gas through the rubber tubing was negligible.

Temperature stability to better than 5 millidegrees at 1.2°, and .04 millidegrees at 4.2°over an hour was thus obtained. At temperatures above the lambda point, to prevent temperature gradients in the bath, the bath was stirred by the input of 7.5 mW of electrical power to a 300 ohm resistor at the bottom of the dewar. This resistor was also used at higher powers to aid in making upward changes of bath temper-

ature, and to boil off any remaining helium at the end of a run.

(c) Temperature Measurement. All bath temperatures were measured with 1cm. bore mercury or butyl-phthalate oil manometers. The vacuum sides of the manometers were pumped with a small rotary pump and the backing pressure read with a Veeco thermocouple gauge.

The manometers were read with a cathetometer calibrated at 20°C. and capable of reading to .005 cm.

The manometers could also be used, (via valve #2), to accurately read or set the pressure in the controller reference volume.

(2) EXPERIMENTAL CHAMBER

(a) Vacuum Can. The experimental chamber and sample mounting are shown in Figure 2. The vacuum can was brass, plated with gold. The two sections were bolted together, the vacuum seal being made with a .050" lead O-ring wiped with vacuum grease. A Consolidated Vacuum Corp. VMF 10 oil diffusion pump working through a liquid nitrogen cold trap evacuated the can through a .25" thin-walled stainless steel pumping line. The pumping line was jogged, and its interior coated with flat black lacquer to prevent room temperature radiation from reaching the thermometers.

The diffusion pump could evacuate the can to a pressure of 10^{-7} torr as measured by a room temperature C.V.C. Phillips gauge between the cold trap and the can.

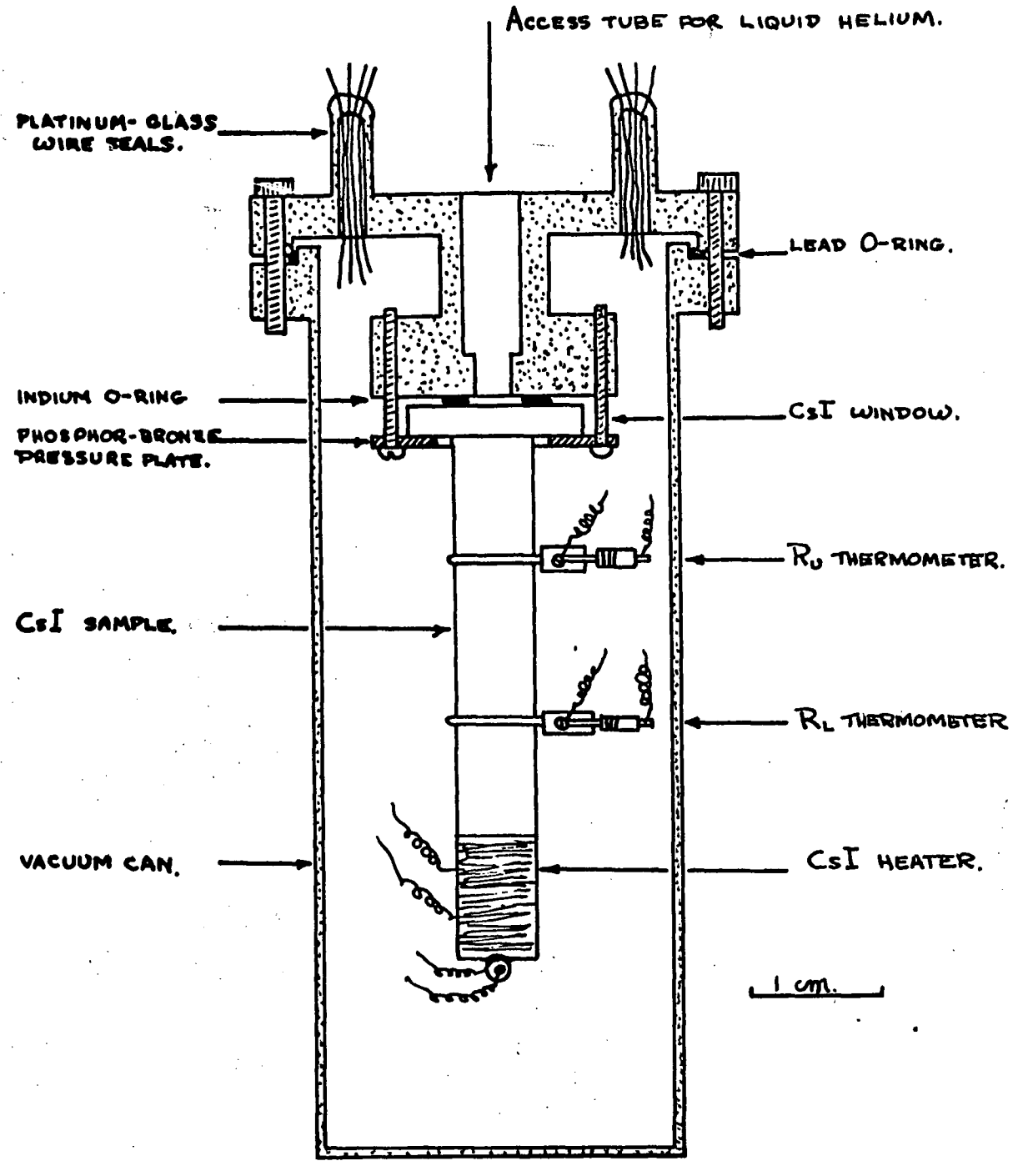

EXPERIMENTAL CHAMBER

FIGURE 2

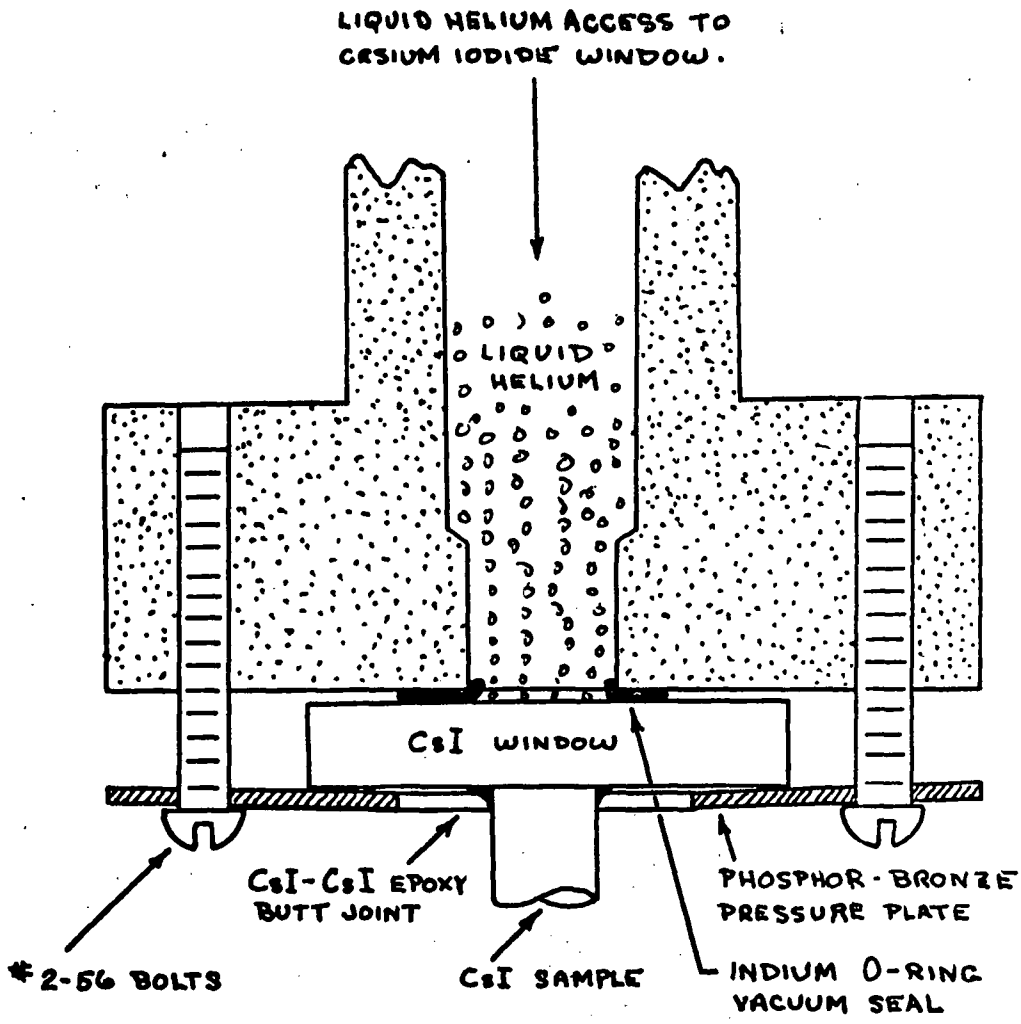

DETAIL: SAMPLE MOUNTING.

FIGURE 3

(b) Samples. The samples were obtained from the Harshaw Chemical Co. and were "optically pure" CsI single crystals. The crystals were machined into rods 3cm. long. The crystal surfaces were not optically flat but had a translucent appearance. Sample sizes were

Sample No.	Length	Diameter D	Thermometer Spacing l
2.	3cm	4.86mm	.944cm
1.	3cm	7.95mm	1.208cm
3.	3cm	2.86mm	.817cm

(c) Crystal Mounting. The major experimental difficulty lay in achieving intimate thermal contact between the sample and the helium bath, a necessity in view of the high heat currents being passed through the sample.

Initially we attempted to make good mechanical contact between the sample and various types of copper holders mounted inside the vacuum can. The efficiency of all of these methods was reduced greatly by the large differential thermal expansion of CsI and copper. The total linear thermal expansion $\Delta L/L$ of CsI from room temperature to helium temperature is 1.16% (James et al, 1965), as compared with 1.13% for Lucite, and .32% for copper.

The best of the mechanical methods consisted of a thin copper foil chuck, tightened around the end of the sample by a tapered Perspex ring. Our hope was that the Perspex ring would keep the copper in good contact with the CsI as it

cooled. This device resulted in an unacceptable sample to bath thermal resistance of about 2500 °K/watt.

The successful solution, suggested by a Kapitza resistance experiment (Johnson et al, 1963), was to insert a CsI window 2-4mm thick, in the top of the vacuum can, and glue the sample to this using an epoxy resin. The seal between the window and the vacuum can was made using a .030" Indium wire O-ring and a circular phosphor-bronze pressure plate (Fig. 3), and was leak tight in liquid helium-II. This system resulted in an acceptable sample to bath thermal resistance of about 50°K/watt.

(d) Sample Heater. In making the sample heater, we were again faced with the difficulty of making good CsI to metal thermal contact. In this case however, the quality of the contact was of lesser importance, poor contact resulting only in a higher heater temperature. If the heater temperature were to rise very high, let us say 20-25°K, some error due to radiation pickup by the thermometers might be encountered. The heater was designed with this possibility in mind.

The heating element consisted of about 20' of .002" constantan wire, with a resistance of about 1250 ohms at helium temperature. A CsI block .5" long and with 5mm square cross-section was cut with grooves perpendicular to its long axis. The heater wire was wound into these grooves

in a matrix of liquid epoxy resin, and the heater block subsequently epoxied to the samples. With this design, the thermometers could not "see" the heater winding. The heater block to sample epoxy resin butt joint had a thermal resistance of around 50°K/watt.

The heater leads inside the can were six inch lengths of .004" constantan wire, with a thermal resistance of 10^6°K/watt, 10,000 times higher than the biggest thermal resistance of the samples. Leads were fed through the vacuum can to the helium bath via a platinum-glass seal.

(e) Thermometers. The thermometers were commercial Allen-Bradley 1/10 watt carbon composition resistors, nominally 33 ohms at room temperature.

Figure 4 shows in detail the mounting of the sample thermometers. A phosphor-bronze spring clip tightened a loop of .45mm diameter copper wire onto the specimen. Tension was increased in the clip by tightening the #000 x 1/8" brass bolt running through it. One lead of the sample thermometer was soldered to the head of this bolt, thus achieving intimate thermal contact between the thermometer and the sample.

Thermometer leads inside the vacuum can were 6" lengths of .004" constantan wire, and were fed through the can via a platinum glass seal separate from the one carrying the heater power. The thermometers were therefore in very bad thermal contact with the bath, as desired.

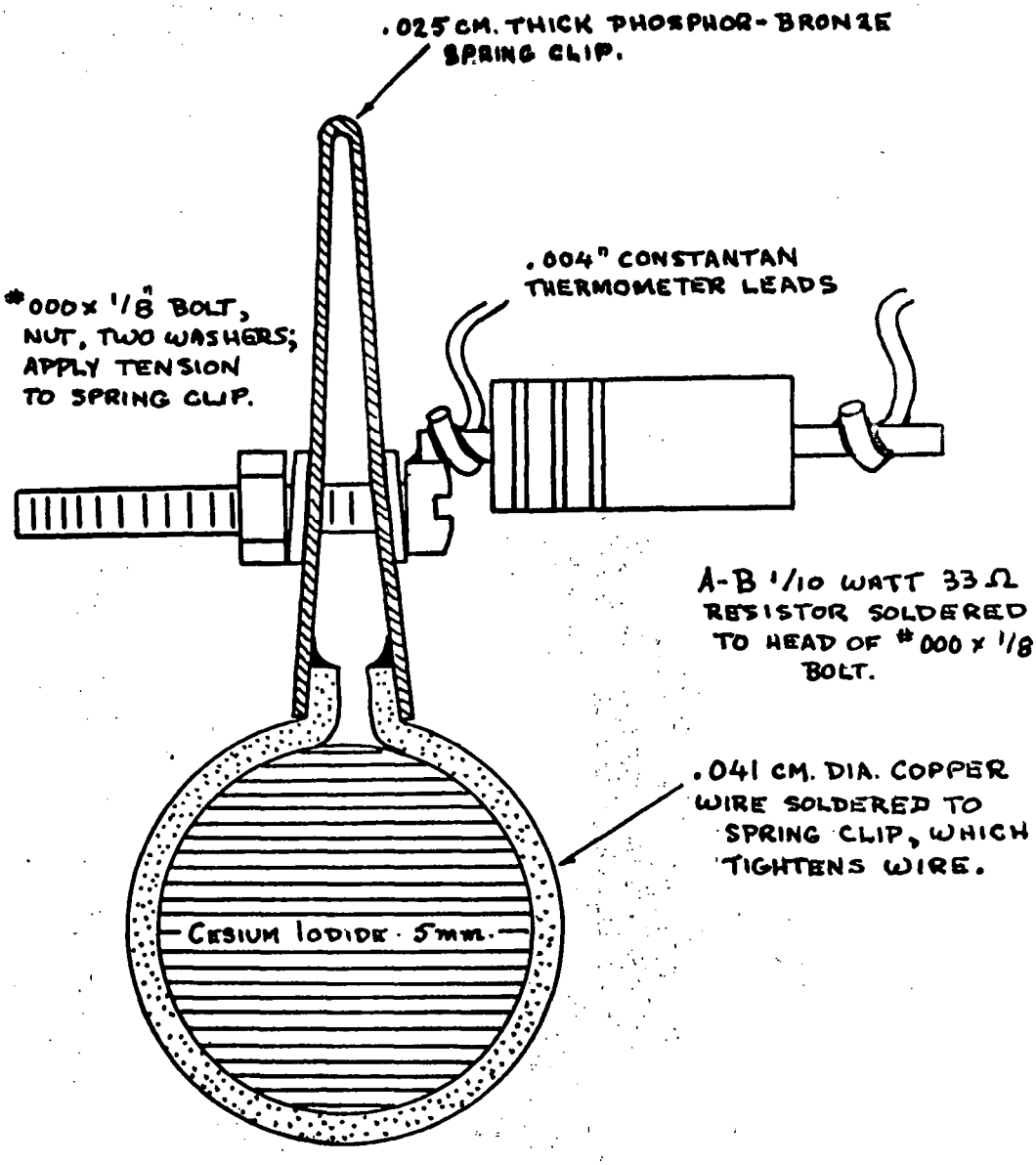

DETAIL: THERMOMETER MOUNTING

FIGURE 4

Two other thermometers were occasionally employed, one held by a copper strap to the interior top of the can and therefore in excellent thermal contact with the bath, and one epoxied to the end of the CsI heater block in order to measure the thermal resistance of the heater block to sample joint.

The two sample thermometers chosen were the two out of twenty whose room temperature resistances were most nearly equal.

(3) ELECTRONICS

(a) Resistance Measurement. Resistances of the thermometers were measured using a sensitive 33Hz AC Wheatstone bridge (Fig. 5). A primary assumption in this experiment is that the sample thermometers are at the same temperature as the sample. This assumption is invalid if the current used to measure their resistance causes appreciable self-heating of the resistors. The power generated in the resistors during measurement was in the range $5\text{-}50 \times 10^{-10}$ watts, insufficient to cause measurable self heating.

(i) Bridge. The resistance thermometers were connected, via co-axial cable and a selector switch, to form the unknown arm of a Leeds & Northrup model 4735 guarded Wheatstone bridge. This has a five decade variable resistance, with an absolute accuracy using all decades, of .25 ohms in, say, 5000. However, since all measurements were comparative,

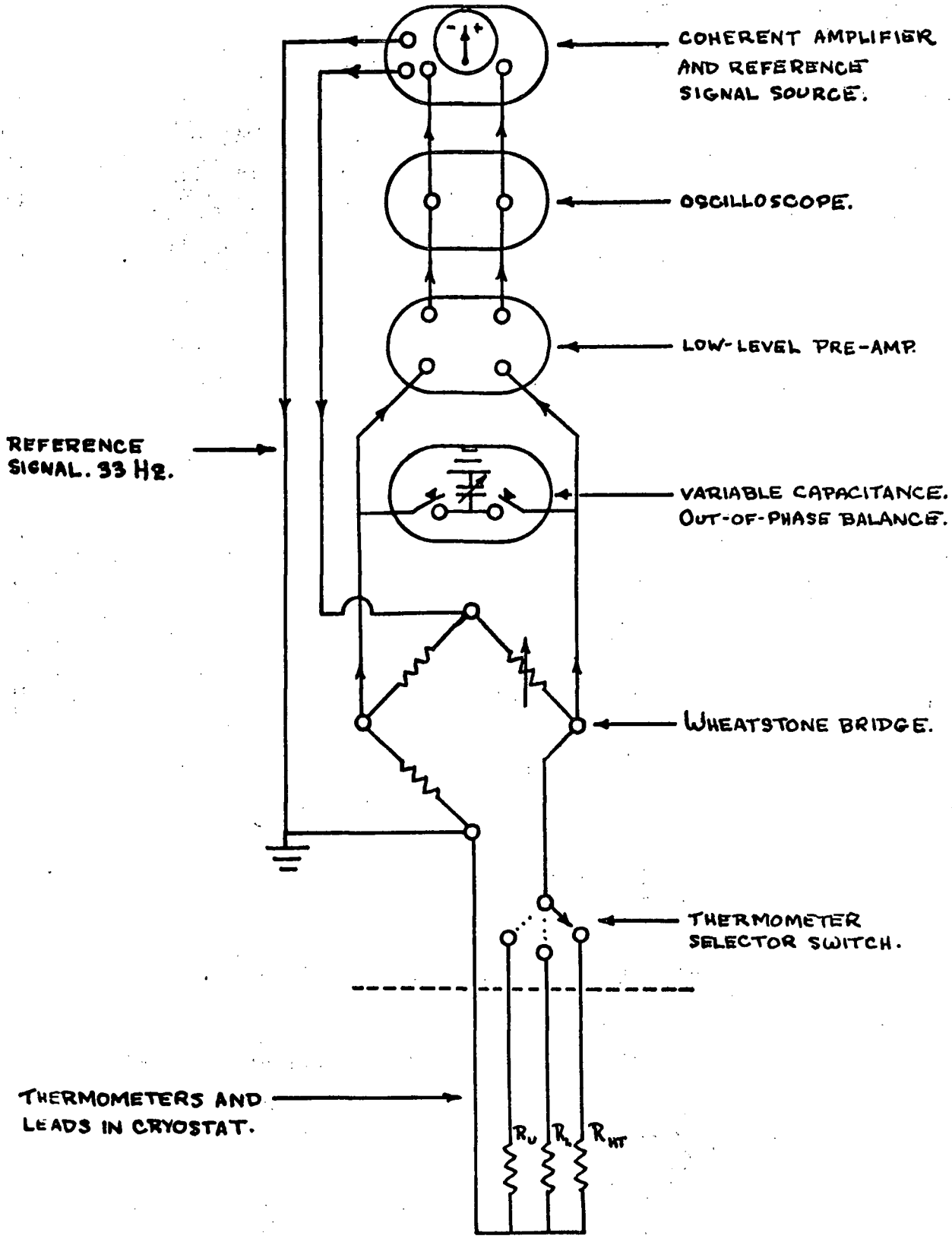

THERMOMETRY ELECTRONICS.

FIGURE 5

using the same bridge under identical conditions, measurements to .01 ohm were quite justified.

(ii) Low-level Preamplifier. The out-of-balance or output signal of the bridge was fed via a shielded cable to a Tektronix type 122 preamplifier. This is an AC-coupled three stage wide-band amplifier with a voltage gain of 1000. It may be powered from an AC power supply, or from dry and wet batteries. As the latter resulted in a significant decrease in noise generation, batteries were used.

The frequency response of the amplifier was decreased as much as possible to improve signal to noise ratio. A low frequency cut-off of 8 Hz and a high frequency cut-off of 50 Hz were used.

(iii) Phase-sensitive Detector. The output of the preamplifier, (ideally just the amplified output of the bridge), was fed to a Teltronics model CA - 2 coherent amplifier. A coherent amplifier is essentially an active filter system which makes use of a priori knowledge of the frequency and phase of its input signal in order to measure its magnitude. The basis of this knowledge is always the fact that the input signal is some function of a reference signal generated by the coherent amplifier.

The reference signal, (33 Hz, 5 volts p-p), was supplied through a 1000:1 voltage reduction as the input to the Wheatstone bridge. A phase control in the coherent amplifier adjusted the detection phase of the input to compensate for phase shifts in the external circuitry, (bridge, coaxial

cables, etc.), so that the signal detected was only the in-phase, or resistive, signal as desired.

The output of the phase sensitive detector was a -500μA to +500μA meter which, when all phase adjustments were correctly made, was directly proportional to the resistive unbalance signal of the Wheatstone bridge, and was therefore the final readout for balancing the bridge. Sensitivity of the system was a deflection of 150μA for an unbalance of 1 ohm in 10,000.

In operation, the zero setting of the meter was discovered to be dependent on the gain and phase shift controls. This was found to be due to the presence of .2mV of reference frequency ripple on the -16 volt B- supply of the input stage transistors. The defect was cured by removing the filtered voltage from the input stages and replacing it with a -15 volt mercury battery.

(iv) Out-of-phase Balance. The coherent amplifier also incorporated a 90° phase shift switch so that the out-of-phase component of the input signal could be measured. An AC bridge is completely in balance only when both in-phase and out-of-phase components are balanced. Out-of-phase balance was accomplished by a variable capacitance to ground in parallel with either the unknown thermometer resistance, or the bridge decade resistance.

(v) Signal Leads. All leads, including those into the cryostat, had to be well shielded due to the low signal levels. With an input voltage to the bridge of 5mV p-p, an out-of-balance of 1 ohm in 10,000 generates an error signal of only .5μV. The noise level at the input to the preamplifier was eventually reduced to 2-5μV random or 60 Hz, but as the signal to noise ratio of the coherent amplifier was approximately 1:1000, a good usable signal was obtained.

Leads were fed through the cryostat cap via a multi-pin shielded plug, vacuum sealed with a layer of Apiezon Q-compound between the pins.

(b) Heater Power Supply. The sample heater was powered by a Harrison Laboratories model 6204A regulated constant voltage 0-36 volt DC power supply, (Fig. 6), remote programmed by a 10-turn Helipot. The desirable features of this power supply were its low ripple (less than .002% at 10 volts) and its high long term stability (better than .15% over eight hours). A voltage divider was used to supply lower voltages to the 1200 ohm sample heater.

(c) Power Measurement. The voltage divider incorporated a circuit for measuring the heater voltage and heater current via a Leeds & Northrup No. 8662 portable precision potentiometer (Fig.6). Reference voltage was supplied by a 1.01940 volt internal standard cell. Each voltage was measurable to 1/4%, the power therefore being accurate to 1/2%.

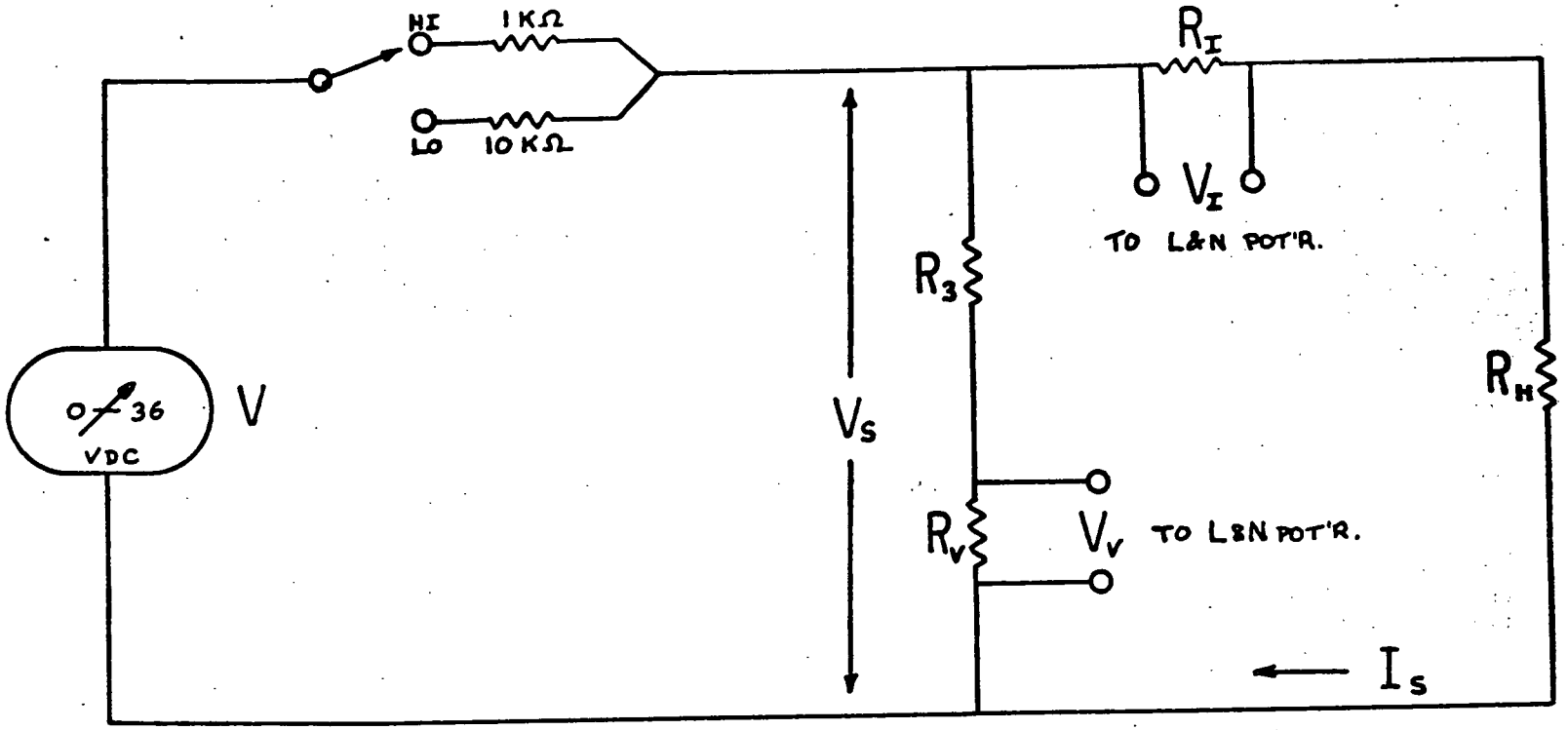

$R_3 = 19,355\ \Omega$

$R_V = 103.69\ \Omega$

$R_I = 4.964\ \Omega$

$P_T = V_S I_S$

$= 37.804 V_V V_I$ mW.

$V_S = 187.66 V_V$ mV.

$I_S = V_I$ mV./4.964 mA

FIGURE 6

DC POWER SUPPLY.

CHAPTER III. PROCEDURE AND TECHNIQUE

(1) INTRODUCTION

Any experiment must be performed under physical conditions rather similar to those implicit in the theoretical treatment it purports to be investigating. Necessary experimental and procedural conditions for this experiment are:

- that the sample be in thermal steady state when any measurements are taken; either under zero heat flow conditions for calibration, or under finite heat flow conditions for conductivity measurements;
- that the thermometers must be in good thermal contact with the sample and bad thermal contact with the helium bath;
- that there be no dependence of the thermometer resistances on the power used to measure them;
- that the measured thermal conductivity at a given temperature must not depend on the power flow through the sample;
- and that no heat generated in the sample heater must reach the helium bath through anything but the sample, whence (a) there must be "no" gas in the experimental chamber, and (b) the sample heater leads must have a thermal resistance large compared with that of the sample.

The design, procedure and technique of the experiment were set up with these factors in mind.

(2) GENERAL EXPERIMENTAL PROCEDURE

A typical run began in the morning. Twenty-fours previous to this, with both dewars at room temperature, the forepump and diffusion pump were turned on, the cold trap filled, and the experimental chamber and vacuum sides of the manometers evacuated.

Some twelve hours later, the helium dewar was pumped out to 1 cm Hg of air, and the nitrogen dewar filled. Thus before any run the experimental chamber was diffusion pumped for about twelve hours at room temperature and twelve hours at nitrogen temperature.

To begin the run, the helium dewar was evacuated, then filled with one atmosphere of helium gas in preparation for the transfer of liquid. The transfer siphon was then flushed with helium gas, the dewar filled with about 3 liters of liquid helium (liquid level about 50cm above the chamber top) and the run begun.

For some runs the experimental chamber was open to the diffusion pump for the duration of the run, while for others it was sealed off just prior to liquid helium transfer to permit cryopumping of the can.

(3) SAMPLE TEMPERATURE MEASUREMENT PROCEDURE: CALIBRATION AND DATA TECHNIQUE

(i) One of the drawbacks of carbon resistance thermometers is that they tend to change their calibration if cycled up to room temperature, then cooled again. In our experience, this change in calibration took the form of an additive constant in the resistance, that constant being nearly the same for both resistors. We feel this fact bears some investigation.

Over the course of several runs, separated by periods at room temperature, one would find shifts in calibration of the thermometers of the order of ± 5 m°K. However, shifts in the difference of the calibrations amounted to only $\pm .5$ m°K and the slopes of the calibration curves remained virtually constant.

In spite of these discoveries, the decision was made that each run should consist of a calibration run and a thermal conductivity run. In practice these were interwoven, a calibration point and a conductivity point taken at one temperature, the temperature then shifted, a calibration point and a conductivity point taken there, and so on.

(ii) Resistance Measurement. The first step in making a resistance measurement was to set up the phase relations of the coherent amplifier so that it was indeed measuring a pure resistance. The procedure was as follows:

(A) Set the bridge decade so that the bridge is definitely out of balance;

(B) With the coherent amplifier at low sensitivity, and in the "in-phase" or φ mode, adjust the phase shift φ to obtain maximum deflection on the output meter.

(C) Obtain a rough resistive balance.

(D) Set the capacitance decade so there is a large capacitive unbalance.

(E) With the coherence amplifier at low sensitivity, and in the "out-of-phase" or $\varphi + 90^\circ$ mode, adjust the $\triangle\varphi$ control to obtain maximum deflection on the meter, thus setting $\triangle\varphi$ to 90°.

(F) Balance the bridge capacitively.

(G) Return to the "in-phase" mode and at high sensitivity, obtain an exact resistive balance.

(H) Check. Apply a large capacitive unbalance. As the coherent amplifier should now be measuring only a pure resistive component, this should have no effect on the meter reading.

Since the phase shift in the external circuitry is largely a property of the geometry thereof, the phase setting procedure need only be followed through once. In fact it was checked occasionally and found not to have changed.

Resistance measurements were taken by simply observing the output meter of the coherent amplifier and adjusting the bridge decades till it read zero.

The bridge contained a multiplier (ratio arm) switch, whose x . 1 (for resistances 300 - 1000 ohms) and x 1.0 (for resistances 1000 - 10,000 ohms) positions were used. The capacitive balance was found to differ on these two ranges, being about + 500 pf on one range and -5000 pf on the other. The capacitance decade was adjusted accordingly.

(iii) Calibration Points. The first step in obtaining a calibration point was to choose the temperature at which it was to be taken. Calibration points were usually planned so as to cover the temperature range of interest in roughly equal intervals of I/T.

Having chosen the temperature, the corresponding vapour pressure was set in the reference volume of the pressure controller. If the result was a drop in temperature, the pumping system quickly pumped the dewar down and a stable temperature was obtained. If, however, the result was a rise in temperature, then the pumping system was shut off by the controller diaphragm. To obtain rapid stabilization, heat was applied to the bath heater until the desired temperature was reached, as indicated by the renewal of gas flow through the pumping system. At all temperatures above the lambda point the bath was continually stirred by a 7.5 mW heat input.

Once bath equilibrium was obtained (usually in 15 seconds to 2 minutes) we waited for thermal steady state of the sample. For the calibration points, an absolute equilibrium

was desired. Thermometer resistances were measured until they were stable over a period of about five minutes. Sample thermal steady state was usually obtained in 20 - 30 minutes.

At such time, the calibration point data were recorded. They consisted of:

(1) time;

(2) R_u, R_ℓ ohms, the resistances of the sample thermometers as measured by the bridge;

(3) h cms, the helium bath level, as measured by metric tape (if bath temperature was above the lambda point);

(4) T-room °C, the temperature of the manometers as measured by thermometer or manotherm (if bath temperature was below the lambda point);

(5) P_{dew} cm Hg or cm oil, the mercury manometer reading if above the lambda point, or the oil manometer reading if below, as measured by the cathetometer;

(6) Check backing pressure<20 microns, as measured by the thermocouple gauge.

This completed the calibration point and one then moved to another calibration point, or to a conductivity point.

(iv) Conductivity Points. Again the first step in obtaining a conductivity point was to choose the temperature at which it was wanted. Having done this, a temperature about .1°K lower was set on the pressure controller and the helium bath brought to this temperature.

Next, heat was generated in the sample heater. This was usually a predetermined amount of heat in the range 0.1 - 3.0 mw, and was set by adjusting the power supply control to the correct value.

We now waited 15 - 30 minutes for thermal steady state. For the conductivity points we were not quite so concerned with absolute steady state (no change in either resistor), but set as our steady state criterion that there be no change in the resistance difference of the two thermometers.

When steady state was obtained, the conductivity point data were recorded. They consisted of:

(1) R_u, R_ℓ ohms, as measured by the bridge;

(2) V_v, V_i mV, as measured by the potentiometer,

the two voltages used in calculating the power in the sample heater.

The measurement of one conductivity point was then complete and one moved on to another conductivity point or to a calibration point.

(v) Power Dependence of Thermal Conductivity. Normally the conductivity points were spaced roughly equally over the temperature range of interest. However, occasionally we wished to know whether the apparent conductivity was dependent on the heat current through the crystal (it should not be). To determine this, a series of points were taken by lowering the bath temperature slightly between each point, and applying enough power to the crystal to bring its temperature up to the temperature at which the first point was measured.

One then obtained a series of conductivity points at roughly equal temperatures but taken with increasing heat currents.

(4) POWER DEPENDENCE OF THERMOMETER TEMPERATURE

As mentioned previously, it is important in this experiment that self-heating of the resistance thermometers due to the measuring current be negligible.

In previous work with carbon resistors the environment of the resistor has been shown to be of importance in determining its self-heating. Clement and Quinnel (1952) found a dependence of temperature rise on power dissipation W given by

$$dW/dT = 2.5 \times 10^{-4} T \quad W/deg$$

for resistors in vacuum in a solid copper heat sink, whereas Berman (1954) found the relationship

$$dW/dT = 3.9 \times 10^{-5} T^{1.6} \quad W/deg$$

for a resistor in vacuum cemented to a copper block in contact with the helium bath.

Due to this strong geometry dependence, we decided to check our thermometers to ensure they were not heating.

A run was done using two temperatures, 4.22°K and 2.10°K. For each temperature, the resistances of the upper and lower thermometers (as well as a "bath thermometer" bolted to the inside of the vacuum can) were measured using power dissipations ranging from 5×10^{-11} watts to 5×10^{-5} watts. The value of R taken at the lowest power was designated as R_o.

The upper and lower resistors behaved in an identical manner and the results for the upper resistor are shown in Table II below, and in Figure 7.

Table II. Thermometer Power Dependence

$T = 4.22°$, $R_o = 377.75$ ohms		$T = 2.10°$, $R_o = 1546.7$ ohms	
R_u/R_{ou}	W watts	R_u/R_{ou}	W
1.000	$.487 \times 10^{-10}$	1.000	2.62×10^{-10}
1.000	1.95 "	1.000	2.84 "
1.000	7.80 "	1.000	11.4 "
1.000	44.8 "	.9996	45.4 "
1.000	48.7 "	.9992	139. "
1.000	195 "	.9980	284. "
1.000	780 "	.9966	1.14×10^{-7}
.9995	4.87×10^{-7}	.9892	4.54 "
.9970	19.5 "	.9456	28.4 "
.9679	78.0 "	-	-
.9424	487 "	-	-

If we assume for the upper resistor a power dependence of the form

$$dW/dT = C\ T^n$$

and if we assume the linear relationship

$$1/T = A + B\ \ln\ (R)$$

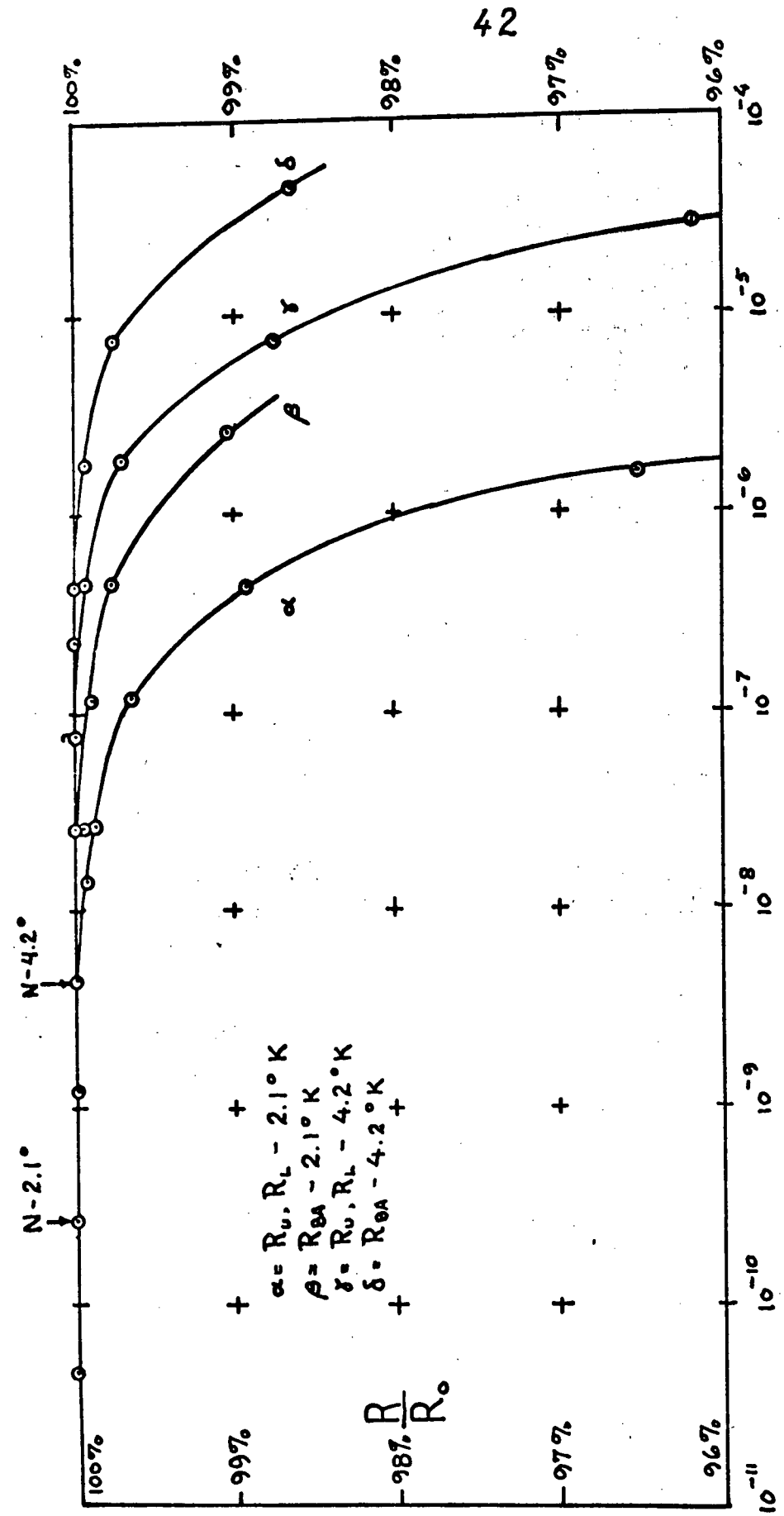

THERMOMETER RESISTANCE VS. MEASURING POWER.

FIGURE 7

for the temperature dependence of the resistance, we then obtain the relationship

$$\frac{dR}{dW} = \frac{-R}{C\,B\,T^{n+2}} \quad .$$

Integrating, we obtain

$$\ln\left(\frac{R}{R_o}\right) = \frac{-W}{C\,B\,T^{n+2}} \quad .$$

From previous calibrations, B is known, and thus using it and the two known temperatures we can solve for C and n. These were found to be

$$C = 1.9 \times 10^{-5} \pm 5\%$$

$$n = 1.99 \pm 5\% = 2 \quad ,$$

giving the relationship

$$dW/dT = 1.9 \times 10^{-5}\, T^2 \quad W/deg$$

for our thermometers.

Knowing the power dissipation to be used in all calibration and thermal conductivity measurements (point N, Fig. 7), and using the derived power dependence relationship we were thus able to show that self heating of our thermometers varied from 1 microdegree at 1.2 °K to about 15 microdegrees at 4.2 °K and was therefore completely negligible.

(5) LEAD RESISTANCES

It will be noted that R_u and R_ℓ refer to the resistances of the upper and lower thermometers plus their associated leads. The calibrations were analyzed in terms of $(R_i - Q_{1i})$ where Q_{1i} are the resistances of the leads.

The last run on each sample was done with the thermometer leads and heater leads short circuited at the thermometers and heater respectively. This was done to determine Q_{1i} (for the thermometers) and also to find what fraction of the total power generated and measured in the sample heater circuit was not dissipated in the heater.

At 4.2°K, the leads constituted about 10% of the total thermometer resistance, and about 3% of the heater resistance. Negligible variation due to bath level or temperature was seen in the resistance of the constantan leads.

(6) SAMPLE GEOMETRY MEASUREMENT

After the low temperature measurements were made, it remained only to establish the geometry of the sample-- its cross-sectional area A, and the distance between the thermometers L.

The diameters D of the sample were measured to 1/4% using a micrometer caliper or a travelling microscope. Center to center distances between the copper wires holding the thermometers were measured to 1/2%, from six directions, using a cathetometer.

CHAPTER IV. DATA REDUCTION

(1) MANOMETRY AND CORRECTIONS

(a) Introduction. All temperatures quoted in this report are based on, but not identical to, the temperatures of the T_{58} helium-4 vapour pressure scale (van Dijk et al, 1960). The 1958 international scale of temperatures is given in terms of the vapour pressure of helium-4 in microns of mercury at 0°C and a standard gravity of 980.665 cm/sec^2.

If vapour pressures are read on finite bore mercury and butyl-phthalate manometers at varying room temperatures and local gravity many corrections must be made to these measured pressures in order to reduce them to accurate T_{58} vapour pressures. We did not consider it necessary to make all these corrections.

We shall define as T_J, the less accurately corrected temperature scale in which we are working. Each thermal conductivity is quoted at a certain temperature. We decided to tolerate an error of up to 1 % in this temperature, i.e. we would tolerate an absolute error between T_{58} and T_J of 10 millidegrees at 1°K and 40 millidegrees at 4°K. The thermal conductivities, however, are inversely proportional to a temperature difference. We decided that an error of .1% could be allowed in this temperature difference, i.e. we would tolerate a difference between some ΔT_J and the corresponding ΔT_{58} of .1%.

(b) Corrections. Suppose some difference in meniscus levels of a mercury or butyl-phthalate manometer has been read with a cathetometer, giving a "raw vapour pressure". Below is a list of all corrections that could be made, and whether in setting up T_J they were, or were not made. Following this section will be a proof that the resulting T_J fulfils its requirements.

Three working criteria were used to determine whether a correction would or would not be retained:

(1) the oil and mercury manometers were to agree to within the 50 micron uncertainty of the cathometometer reading,

(2) if a correction factor was time independent it was ignored, and

(3) if a correction factor was always less then the 50 micron cathetometer uncertainty it was ignored.

The corrections are:

(i) Backing pressure. The pressure in the vacuum side of the manometers was always checked. It was always greater than 1 micron and less than 10 microns and was therefore ignored.

(ii) Meniscus errors arise if the meniscuses on the two arms of the manometer are of different shapes. Since the "height" of a mercury meniscus (the vertical distance from the center point of the column to the point at which it touches the walls of the tube) is typically 1000 - 1500

microns for a 1 cm bore tube, this error can be large. The manometers were therefore tapped well before each reading. Experience showed that this brought the meniscus error to within the 50 micron cathetometer uncertainty, and the correction was ignored.

(iii) Thermal expansion of cathetometer. The cathetometer was calibrated at 20°C, and had a thermal expansion coefficient of 1.2×10^{-5}/°C. Maximum error from this source would occur at a bath temperature of 4.2°K, and at the highest room temperature, say 24°C. Under these worst conditions the error is 40μ. Cathetometer expansion was therefore ignored.

(iv) Hydrostatic head correction. The measured vapour pressure was that of the surface of the helium bath whereas the thermometers were as much as 50 cm below this point and hence the liquid surrounding them was at a higher pressure. Maximum error from this source is about 4000 microns and is time dependent. It is therefore included.

(v) Gravity. The pressure exerted by a column of mercury is directly proportional to the acceleration of gravity. The value taken for local gravity (980.937 cm/sec^2) was from a Department of Mines and Technical Surveys measurement taken within 100 yards of the experiment. The ratio of this value to the T_{58} standard gravity is

$$\frac{980.937}{980.665} = 1.00028$$

giving a maximum error in vapour pressure at 4.2°K of about

220 microns. However, the error is time-independent and is therefore ignored.

(vi) Density, (A) of mercury due to constant room temperature. The T_{58} scale is in terms of mercury at 0°C. If we assume for T_J a constant room temperature of, say, 23°C, we introduce an error in the density of mercury of $\rho(23)/\rho(0) = .99583$ or an error of .417%. This results in a maximum pressure error of about 3500 microns. As we have assumed a constant room temperature, however, the error is time-independent and is therefore ignored.

(B) of mercury due to variable room temperature. Here we account for the falsity of the previous assumption of constant room temperature. If the room temperature were to vary rather rapidly, there would be an apparent variation in bath temperature due to the variation in mercury density. We introduce an additional criterion at this point, that the apparent change in bath temperature shall not exceed 1/2 millidegree/hour. The situation is worst at the lowest temperature of 1.2°K (since the quantity $(dP_V/dT_{BA})/P_V$ is largest there) and our calculation is for a helium bath at that temperature.

At 1.2°K the vapour pressure of helium-4 is 625 microns. The slope of the vapour pressure curve dP_V/dT_{BA} is 4.41 microns/millidegree. The volumetric expansion coefficient of mercury at room temperature is $\beta = .85 \times 10^{-3}/°C$. Using these values, it is easy to show that an apparent bath temp-

erature variation of 1/2 millidegree/hr requires a room temperature variation of at least 4°C/hour. Changes of room temperature of this rate were never observed therefore this correction is ignored.

(C) Ratio of mercury to butyl-phthalate.

There must be no discontinuity when going from the mercury manometer to the oil manometer. The ratio of the density of butyl-phthalate to the density of mercury must therefore be known accurately, as a function of room temperature. We could find no published data on this ratio, therefore we performed a short, accurate experiment to establish $\rho_{oil}(T)$, and $\rho_{oil}(T)/\rho_{Hg}(T)$ for temperatures between 15°C and 25°C. The results of this experiment are shown in Appendix 1.

A thermometer was then constructed using butyl-phthalate as the thermometric substance, with a long tubular bulb, the shape of half a manometer. This device, which we call a "manotherm" was used to read room temperature, on the assumption that its thermal response time most closely matched that of the manometers.

This correction is necessary and is therefore included.

(2) T_J vs. T_{58}.

The helium-4 vapour pressure scale T_{58} is a relationship between temperature and pressure defining a correspondence f(p);

$$T_{58} = f(P_{58}).$$

As shown in the previous section, vapour pressures for

the T_J scale are obtained by measuring the dewar pressure P_{dew} under existing conditions, and making a head correction where necessary;

$$P_J = P_{dew} + \text{head correction, whence } T_J = f(P_J).$$

The T_{58} scale vapour pressures, P_{58} are obtained from P_{dew} by including the effects of backing pressure, local gravity and room temperature;

$$P_{58} = P_{dew} + \text{gravity correction} + \text{cathetometer expansion} + \text{room temperature correction} + \text{backing pressure} + \text{head correction.}$$

We now wish to observe, for a typical set of measuring conditions, the difference between T_J and T_{58}. We will assume a backing pressure of 5 microns, a varying room temperature of 22°C ± 2°C, a local gravity of 980.937 cm/sec^2, and for simplicity, a zero head correction. Under these conditions, the corrections are

(a) Backing pressure. . . . . + 5 microns

(b) Gravity . . . . . + $(.277) \times 10^{-3} P_{dew}$ microns

(c) Room temperature. . . - $(3.99 \pm .36) \times 10^{-3} P_{dew}$ microns

(d) Cathetometer. . . . + $(.024 \pm .024) \times 10^{-3} P_{dew}$ microns

(e) Head correction. . . . . 0 microns

giving a total correction of

. . . . . - $(3.69 \pm .38) \times 10^{-3} P_{dew}$ microns.

For the conditions above we see, therefore,

$$P_J = P_{dew}$$

$$P_{58} = P_{dew} - (3.69 \pm .38) \times 10^{-3} P_{dew} + 5 \text{ microns.}$$

Using selected values of P_{dew} we have prepared Table III below, comparing $T_J = f(P_J)$ and $T_{58} = f(P_{58})$.

Table III

T_{58} °K	T_J °K	$T_J - T_{58}$ m°K
4.5000	4.5042 ± .0004	4.2 ± .4
4.0000	4.0037 ± .0004	3.7 ± .4
3.5000	3.5030 ± .0003	3.0 ± .3
3.0000	3.0024 ± .0003	2.4 ± .3
2.5000	2.5018 ± .0012	1.8 ± .2
2.0000	2.0012 ± .00013	1.2 ± .13
1.5000	1.5005 ± .00008	.5 ± .08

These results are plotted in Figure 8, from which it may be seen that for T greater than 1.5°K, the relationship between $T_J - T_{58}$ and T_{58} is linear, of the form

$$T_J - T_{58} = m T_{58} + b.$$

Such being the case, let us assume a $\Delta T_{58} = T_{58}(1) - T_{58}(2)$, and a corresponding ΔT_J.

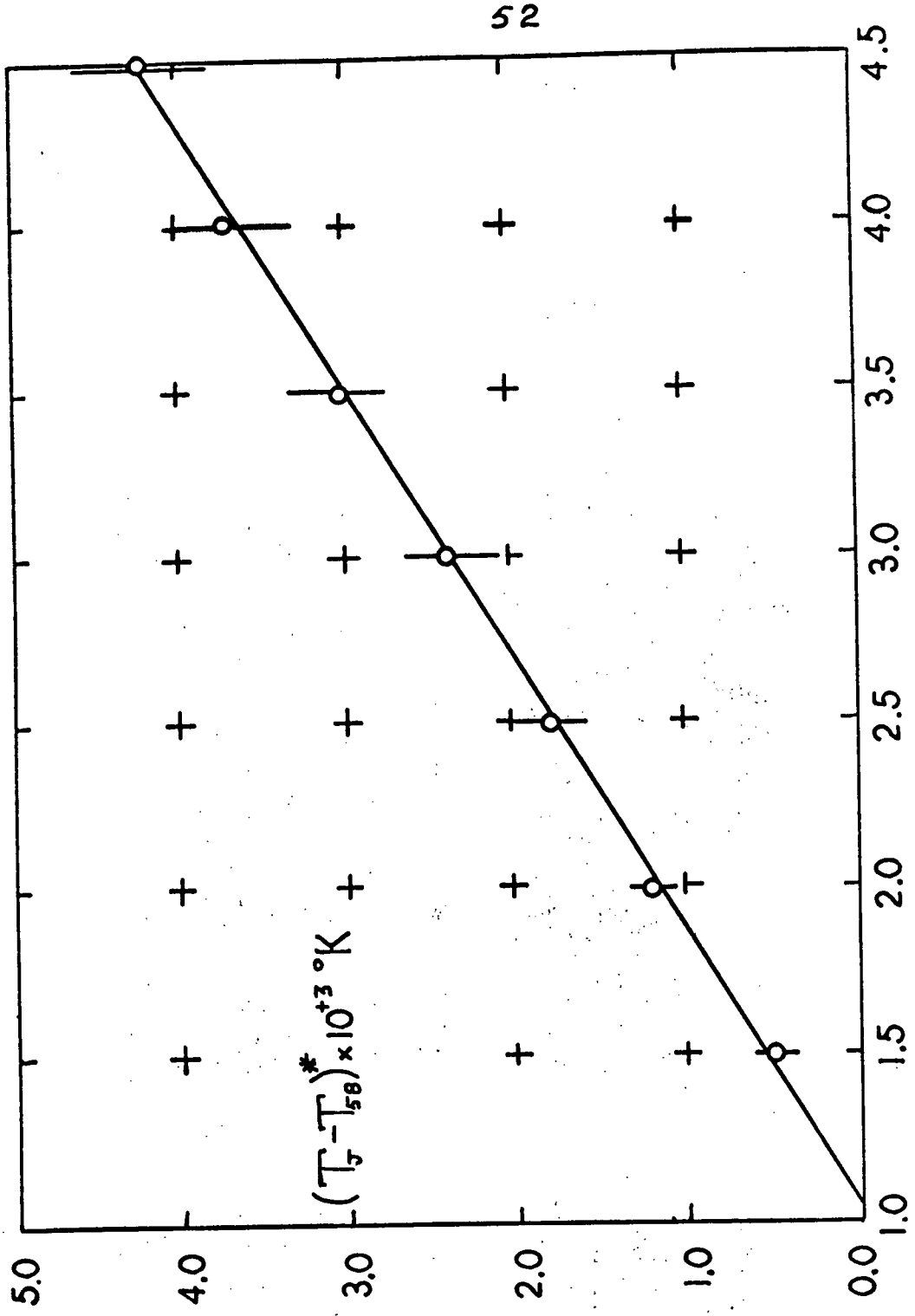

$T_T - T_{58}$ VS T_{58}

* (CALCULATED FOR VARIABLE ROOM TEMPERATURE OF 22°C ± 2°C.)

FIGURE 8

We therefore write

$$T_J(1) - T_{58}(1) = m\, T_{58}(1) + b,$$

$$T_J(2) - T_{58}(2) = m\, T_{58}(2) + b,$$

and subtracting,

$$T_J(1) - T_{58}(1) - T_J(2) + T_{58}(2) = m\,(\,T_{58}(1) - T_{58}(2)\,)$$

or

$$\Delta T_J - \Delta T_{58} = m\, \Delta T_{58}\,.$$

From the graph we obtain a slope (using maximum and minimum values) of $m = .0012 \pm .0001$.

It may be seen from the graph that the largest absolute error occurs at the highest temperature, say $4.5^{\circ}K$.

Putting in the appropriate figures, we obtain an absolute error

$$\frac{T_J - T_{58}}{T_{58}} \leqq .1\% < \text{required } 1\%,$$

and a fairly constant relative error

$$\frac{\Delta T_J - \Delta T_{58}}{\Delta T_{58}} = .12\% \cong \text{required } .1\%$$

Hence we see that the T_J temperature scale does indeed fulfil its requirements and we conclude that we are justified in its use.

(3) CALIBRATION PROCEDURE AND PROGRAM.

Once a set of calibration points (R,T) is obtained for a given thermometer on a given run, some method of mathematical interpolation must be found to make it useful. One

wishes to find that analytic expression which best describes the observed temperature dependence of the resistor. To facilitate this, a computer was used to perform least squares fits of the input data to various analytic expressions.

(a) Input data. Consisted of:

- N, the number of calibration points,
- (R), the N values of resistance measured on the bridge,
- (T), the N corresponding calibration temperatures as calculated in the previous section, and
- Q_L, the resistance of the thermometer leads, since $R-Q_L$ is the resistance of the thermometer alone. This input data is of course pertinent to only one resistor.

(b) Calculation. Using the above data, a single iteration least squares fit was performed to each of the following expressions.

- LINEAR

$$1/T = A_1 + B_1 \ln(R-Q_L),$$

- QUADRATIC

$$1/T = A_2 + B_2 \ln(R-Q_L) + C_2 \ln^2(R-Q_L),$$

- CUBIC

$$1/T = A_3 + B_3 \ln(R-Q_L) + C_3 \ln^2(R-Q_L) + D_3 \ln^3(R-Q_L),$$

- CUBIC + 1/LOG R

$$1/T = A_4 + B_4 \ln(R-Q_L) + C_4 \ln^2(R-Q_L) + D_4 \ln^3(R-Q_L) + E_4 / \ln(R-Q_L),$$

- CUBIC + 1/LOG R + 1/(LOG R)**2

$$1/T = A_5 + B_5 \ln(R-Q_L) + C_5 \ln^2(R-Q_L) + D_5 \ln^3(R-Q_L) + E_5 / \ln(R-Q_L) + F_5 / \ln^2(R-Q_L).$$

For each expression, the intermediate estimate of the parameters $(A, \ldots, F)$ consisted of the final estimate of the parameters of the previous expression, the intermediate estimate for the linear case being $A = 0$, $B = 0$.

For each expression, when the final estimate of parameters was obtained, it was used to calculate the set $|1/TFIT|$ -- the inverse temperatures corresponding to the input set R and the estimated parameters. The inverse temperatures 1/T from the input set T were also calculated.

Finally, for each set of parameters, a set of numbers called "TYPE 2 ERRORS" was calculated.

(c) Output. For each expression (linear, quadratic, etc.) the output consisted of:

- Name of expression (linear, etc.),
- Intermediate estimate of parameters

  A, B, C, D etc.,
- Final estimate of parameters

  A, B, C, D, E, etc.,
- Set of N values for

R	T	R-Q	1/T	1/TFIT	LOG(R-Q)
-	-	-	-	-	-
-	-	-	-	-	-
-	-	-	-	-	-

- "TYPE 2 ERRORS".

(d) Analysis. For each thermometer on each run we were thus presented with five possible analytic expressions describing its behaviour. It remained only to pick the best one. There were two criteria for the best fit;

(i) the average value of the set $|1/T - 1/TFIT|$ must be as small as possible, and

(ii) the "TYPE 2 ERROR" corresponding to each parameter should be less than 10% of the magnitude of the parameter.

In practice the $|1/T - 1/TFIT|$ average was relatively high for the LINEAR FIT ($5\text{-}10 \times 10^{-3}$), about two orders of magnitude lower for the QUADRATIC FIT ($5\text{-}10 \times 10^{-5}$), and showed little if any improvement for higher order expressions. The "TYPE 2 ERRORS" rose with increasing order of expressions and generally exceeded 10% of the corresponding parameter at the CUBIC.

The optimum fit was nearly always the QUADRATIC, and occasionally the CUBIC. The LINEAR, CUBIC + 1/LOG R, and CUBIC + 1/LOG R + $1/(\text{LOG R})^2$ expressions were never selected.

Magnitudes of a typical set of parameters for the upper resistor are

$$A = -0.27476$$

$$B = +0.033491$$

$$C = +0.0093272$$

$$D = 0$$

$$E = 0$$

$$F = 0$$

(4) CONDUCTIVITY POINT ANALYSIS; T.ΔT PROGRAM.

On a given run, the raw data for conductivity points consisted of the set of quadruplets (R_u, R_l, V_v, V_i) -- the resistances of the upper and lower thermometers, and the two voltages from the power measurement circuit (chap. III - 3). From these one must obtain the heat current or power through the sample, and the temperature difference between the thermometers.

(a) Heat current. (Fig. 6) Define V_s as the voltage applied to the sample heater, leads, and current measuring resistor. Then the measured potential V_v is proportional to V_s,

$$V_s = \frac{(R_3 + R_v)}{R_v} V_v .$$

Define I_s as the current through the sample heater, leads, and current measuring resistor. Then the measured potential V_i is proportional to I_s,

$$I_s = \frac{V_i}{R_i} .$$

But the total power P_t generated in the sample heater, leads and current measuring resistor is just

$$P_t = V_s I_s$$
$$= \frac{(R_3 + R_v)}{R_v R_i} V_v V_i .$$

If we assume that all the power generated in the sample heater is delivered to the sample, and all the power generated in the leads and current measuring resistor is dissipated

elsewhere, then the ratio of power through the sample P, to total power P_T, is just the ratio of the average resistance of the sample heater at low temperature R_{HT}, to the total circuit resistance $R_{HT} + R_{HTL} + R_i$. R_{HTL} is the resistance of the leads, R_i the resistance of the current measuring resistor.

$$\frac{P}{P_T} = \frac{R_{HT}}{\left(R_{HT} + R_{HTL} + R_i\right)} \quad \text{or}$$

$$P = \frac{R_{HT}}{(R_{HT} + R_{HTL} + R_i)} P_T ,$$

but we know P_T, therefore we obtain the final expression for the power through the sample,

$$P = \frac{R_{HT}}{(R_{HT} + R_{HTL} + R_i)} \cdot \frac{(R_3 + R_v)}{R_v R_i} \quad (V_v V_i).$$

All resistances have been measured, and thus the heat current is proportional to the measured voltages V_v, V_i.

Values of the resistances, for the 8mm sample, are shown below, together with a typical value of V_v and V_i.

R_3 = 19,355 ohms

R_v = 103.69 ohms

R_i = 4.964ohms

R_{HT} = 1216.3 ohms

R_{HTL} = 38.28 ohms, and therefore

$P = 36.507\ V_v V_i$.

Typically V_v = 6.953 mV, V_i = 5.239 mV giving

$P = 36.507\ (6.953 \times 10^{-3})\ (5.239 \times 10^{-3})$ watts

= 1.330 mW, a typical value for the power through the sample.

(b) Temperature difference ΔT, is the temperature difference between the upper and lower resistors,

$$T = T_L - T_U .$$

From the calibration program we have obtained the parameters for the relations

$$1/T_U = A_U + B_U \ln(R_U - Q_{LU}) + C_U \ln^2(R_U - Q_{LU}) + D_U \ln^3(R_U - Q_{LU}),$$

$$1/T_L = A_L + B_L \ln(R_L - Q_{LU}) + C_L \ln^2(R_L - Q_{LU}) + D_L \ln^3(R_L - Q_{LU}).$$

A simple program was therefore designed to calculate the temperatures of the upper and lower resistors, and their temperature differences.

(i) Input data. Consisted of, for each resistor;

- N, the number of resistance values,
- Q_L, the lead resistance for that resistor,
- Parameters, the set (A, B, C, D, E, F) for that resistor,
- Set (R) of N resistance values.

(ii) Output data. Consisted of;

- T_U, the calculated temperatures of the upper thermometer,
- T_L, the calculated temperatures of the lower thermometer,

- $\Delta T = T_L - T_U$, the temperature differences between the two thermometers.

As well as the (R_U, R_L) pairs for the conductivity points (i.e. the resistance pairs taken while power was flowing through the sample), the original calibration point pairs were fed to the T, ΔT program. In theory, since these points were used to produce the calibration parameters, and were taken under zero heat current conditions, all ΔT corresponding to these resistances should be zero. In practice therefore, the ΔT calculated from these resistances are a measure of the total error in calibration, program calculations, and roundoff. These ΔTs generally averaged 0.1 or 0.2 millidegrees.

ΔTs used for conductivity measurements ranged from 1 to 15 millidegrees.

(5) CONDUCTIVITY CALCULATION.

We have already calculated the power P through the sample and the temperature difference ΔT between the thermometers (chap. IV - 4). The distance L between the thermometers, and the diameter D of the sample have been measured (chap. III - 6).

The thermal conductivity k in terms of the power, temperature difference, thermometer spacing and cross-sectional area of the sample is

$$k = \frac{P}{\Delta T} \cdot \frac{L}{A} \quad ,$$

and $$A = \frac{\pi D^2}{4} \quad ,$$

whence $$k = \frac{P}{\Delta T} \frac{4L}{\pi D^2} \quad .$$

The temperature T at which the conductivity was measured was taken to be

$$T = \frac{T_U + T_L}{2} \quad ,$$

the average temperature between the thermometers.

Finally, substituting expressions for P and ΔT, we obtain the thermal conductivity

$$k = \frac{R_{HT}}{(R_{HT} + R_{HTL} + R_i)} \cdot \frac{(R_3 + R_v)}{R_v R_i} \cdot \frac{(V_v\ V_i)}{T_L - T_U} \cdot \frac{4L}{\pi D^2}$$

at temperature $$T = T_L - T_U \,/\, 2,$$

or $$k = G \frac{V_v\ V_i}{T_L - T_U} \quad ,$$

where G is a known constant for a given sample.

CHAPTER V. RESULTS AND INTERPRETATION

(1) PRESENTATION OF RESULTS

(a) Data. Data for the thermal conductivity calculations on the three CsI samples were gathered from a series of about eighteen liquid helium runs. The measured thermal conductivities for the samples are shown in Tables IV, V and VI, and in Figure 9.

(b) Errors. The major uncertainties and error bars of the conductivity values result from the uncertainty in the measured ΔT's used to calculate them. The average of the moduli of the ΔT's calculated for the calibration points on a given run was taken to be the uncertainty in all ΔT's for that run (see Chap. 4 sec. 4-b). The total uncertainty in the thermal conductivity introduced by the measurements of power and sample geometry is about 1%.

Note, however, that there is a systematic error present. Sample geometry was measured at room temperature. The total thermal contraction of CsI from room temperature to helium temperature is 1.16% (James et al, 1964) and the ratio L/A should therefore be increased by 1.16% if its low temperature value is to be used in conductivity calculation. The conductivity values calculated here are based on the room temperature value of L/A and are therefore low by 1.16%.

TABLE IV

Thermal Conductivity of Sample # 1.

Room Temperature Diameter D = .795 cm

T°K	k watt/cm°K	T°K	k watt/cm°K
4.33	4.40 ± 0.6	1.79	.943 ± .04
4.27	4.32 ± 0.6	1.75	.843 ± .05
3.81	5.98 ± 1.5	1.74	.928 ± .03
3.46	4.13 ± 0.6	1.68	.717 ± .02
3.44	3.59 ± 0.3	1.62	.642 ± .01
3.11	7.34 ± 2.0	1.55	.593 ± .05
2.92	3.88 ± 0.5	1.54	.552 ± .02
2.69	2.88 ± 0.3	1.52	.595 ± .02
2.38	1.55 ± 0.1	1.51	.542 ± .01
2.21	1.44 ± 0.1	1.45	.571 ± .05
2.01	1.39 ± 0.1	1.40	.476 ± .02
1.90	.965 ± .03	1.37	.471 ± .04
1.89	1.04 ± .05	1.34	.459 ± .02
1.86	.977 ± .04	1.29	.411 ± .04

TABLE V

Thermal Conductivity of Sample # 2

Room Temperature Diameter D = .486 cm

T°K	k $\frac{\text{watt}}{\text{cm °K}}$
5.41	6.04 ± .64
4.17	1.79 ± .13
4.15	2.00 ± .16
4.16	1.94 ± .13
4.03	1.83 ± .15
2.90	.819 ± .01
2.69	.707 ± .01
2.59	.656 ± .008
2.58	.742 ± .01
2.41	.630 ± .01
2.10	.492 ± .01
1.97	.384 ± .005
1.96	.397 ± .005
1.57	.229 ± .005
1.48	.196 ± .003
1.41	.177 ± .003
1.26	.131 ± .003

TABLE VI

Thermal Conductivity of Sample # 3*

Room Temperature Diameter D = .286 cm

T °K	k $\frac{\text{watt}}{\text{cm °K}}$
4.34	1.13 ± .02
4.26	.778 ± .10
4.06	.867 ± .01
3.52	.825 ± .10
3.08	.459 ± .02
3.05	.488 ± .05
2.49	.246 ± .01
2.21	.198 ± .003
2.14	.163 ± .003
2.10	.154 ± .002
2.05	.153 ± .002
1.94	.128 ± .002
1.85	.110 ± .002
1.75	.0974 ± .002
1.73	.0938 ± .002
1.63	.0797 ± .002
1.52	.0659 ± .001
1.44	.0573 ± .001
1.42	.0567 ± .001
1.17	.0339 ± .001

* Note: Sample #3 is sample #1 ground down from .795 cm to .286 cm by abrading with a high speed grinding tool.

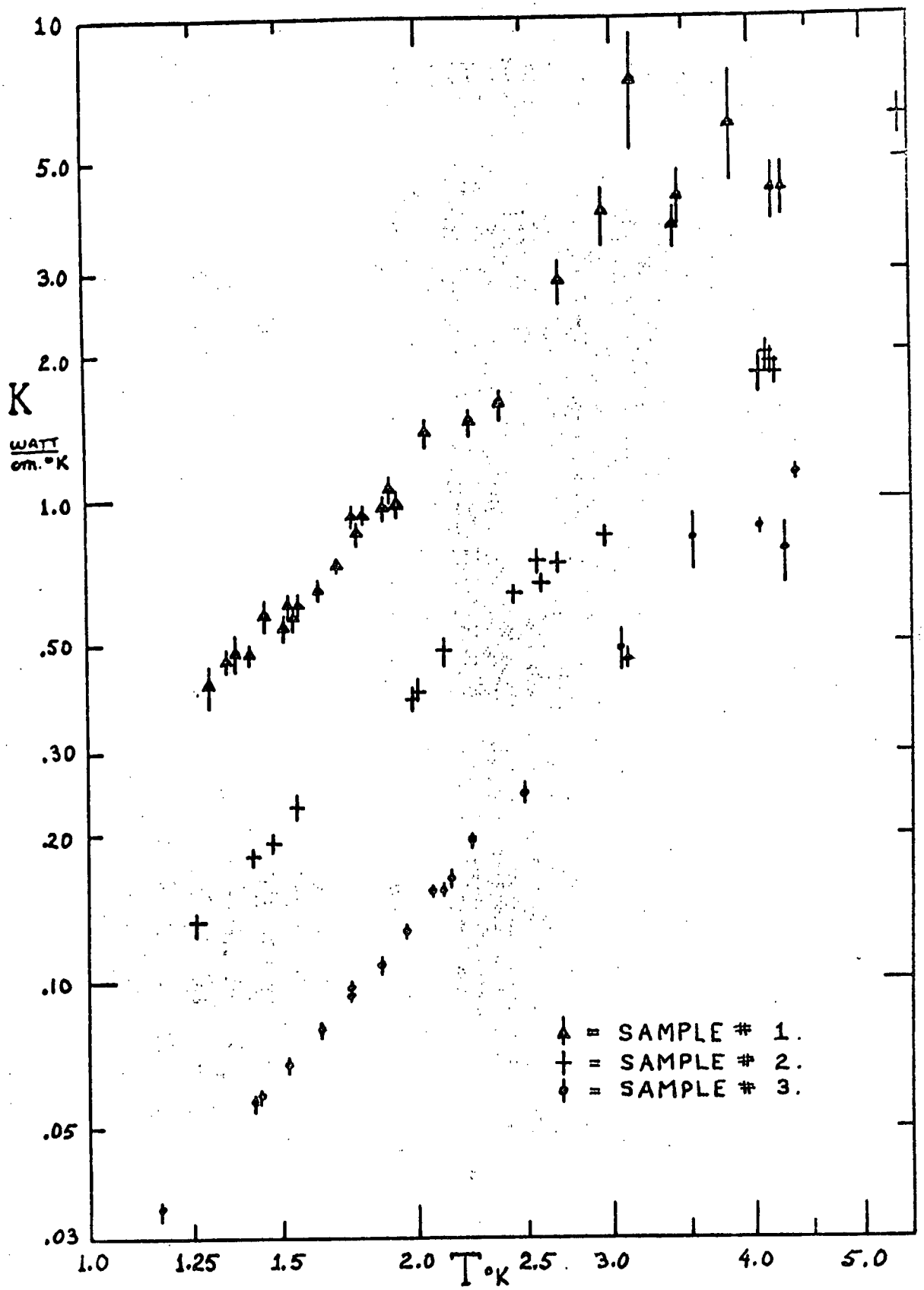

THERMAL CONDUCTIVITY OF CsI.

FIGURE 9

(c) Graphical Analysis. When the points had been plotted on a log-log graph (Fig. 9) they seemed to suggest the existence of one straight line relationship for each sample, and the existence therefore of a relationship of the form $k = AT^n$ for each sample. Graphical determination of these best straight lines led to the following results;

Sample #1. $k = A_1T^{n_1}$, where

$A_1 = .19 \pm .02$, and

$n_1 = 2.61 \pm .1$ ---------- (1),

Sample #2. $k = A_2T^{n_2}$, where

$A_2 = .072 \pm .008$, and

$n_2 = 2.45 \pm .1$ ---------- (2),

Sample #3. $k = A_3T^{n_3}$, where

$A_3 = .022 \pm .002$, and

$n_3 = 2.69 \pm .1$ ---------- (3).

(2) INTERPRETATION OF RESULTS

(a) Size Dependence. The thermal conductivity is different for each of the three samples, thereby suggesting the presence of a size-dependent thermal conductivity. When boundary scattering is the sole phonon scattering mechanism, theory predicts a conductivity $k = BDT^3$, where B is some constant. A graph of k/T^3 vs. diameter D for the various samples should

therefore yield a straight line of slope B passing through the origin.

As the accuracy of the data improves markedly below the lambda point, it was decided to average k/T^3 for each sample for $T \leqq 2.1°K$. The average values of k/T^3 for each sample are shown in Table VII below, together with the standard deviation of the value of k/T^3.

TABLE VII

Sample #	$(k/T^3) \pm \sigma, (T \leqq 2.1°K)$	D_{cm}
1	$.166 \pm .016$	.795
2	$.0578 \pm .0062$	.486
3	$.0185 \pm .0013$	.286

These results are shown in Figure 10. It may be seen that the points do <u>not</u> lie on a straight line through the origin, and in fact the three points cannot be made to lie on a straight line at all. The points seemed to suggest a parabola of the form $(k/T^3) = B' D^2 T^3$ and it was therefore decided to plot k/T^3 vs. D^2. This plot is also shown in Figure 10.

These three samples appeared to give a size dependence proportional to D^2, and a temperature dependence somewhat less than T^3. We therefore used a graphical method to obtain

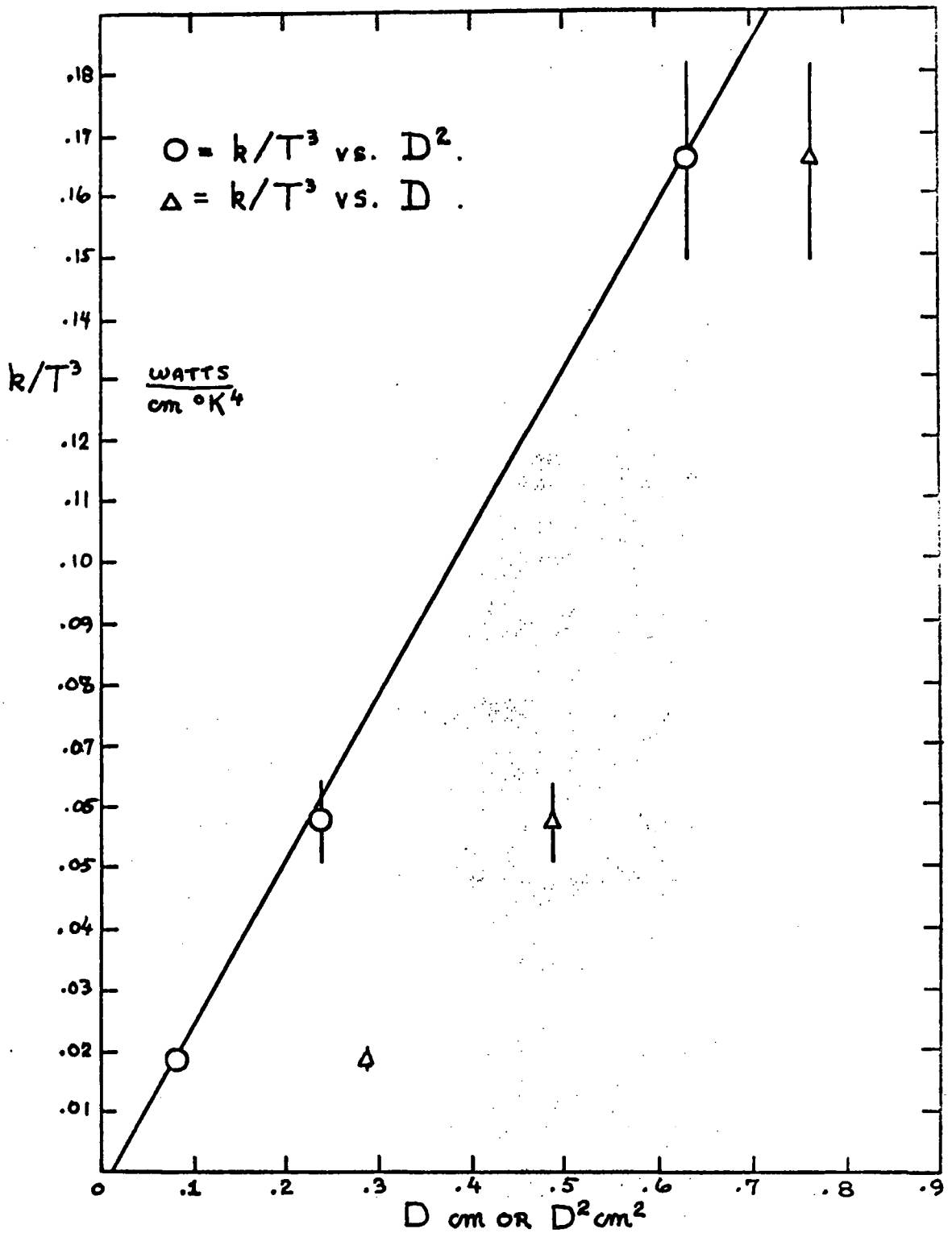

SIZE DEPENDENCE - A

FIGURE 10

an empirical equation for the behaviour of all three samples, of the form $k = B' D^2 T^n$. The result obtained was

$$k = (.31 \pm .02)\ D^2 T^n \text{ watt/cm°K, where}$$

$$n = 2.58 \pm .1 \quad \text{---------- (4).}$$

The graph of k/D^2 vs. T is shown in Figure 11.

Now let us compare these results with the conductivity predicted theoretically on the assumption that scattering from the sample walls is the only phonon scattering mechanism. If k_o is the theoretical thermal conductivity, then from above (Chap. I, sec. 4 - d) we have

$$(k_o/T^3) \cong 1.65\ D \text{ watt/cm°K}^4 \quad \text{---------- (5).}$$

If we evaluate 1.65 D for the three samples, then compare this with the experimental values of (k/T^3) from Table VII, we obtain the following ratios of measured to predicted thermal conductivity;

Sample #1 $(k/k_o) = 12.7\%$

Sample #2 $(k/k_o) = 7.2\%$

Sample #3 $(k/k_o) = 3.9\%$ ---------- (6).

This is a very large discrepancy between theory and experiment. We therefore concluded that boundary scattering from the walls is not the major phonon scattering mechanism. This conclusion is also borne out by the temperature dependence of about $T^{2.6}$. Pure boundary scattering would lead to

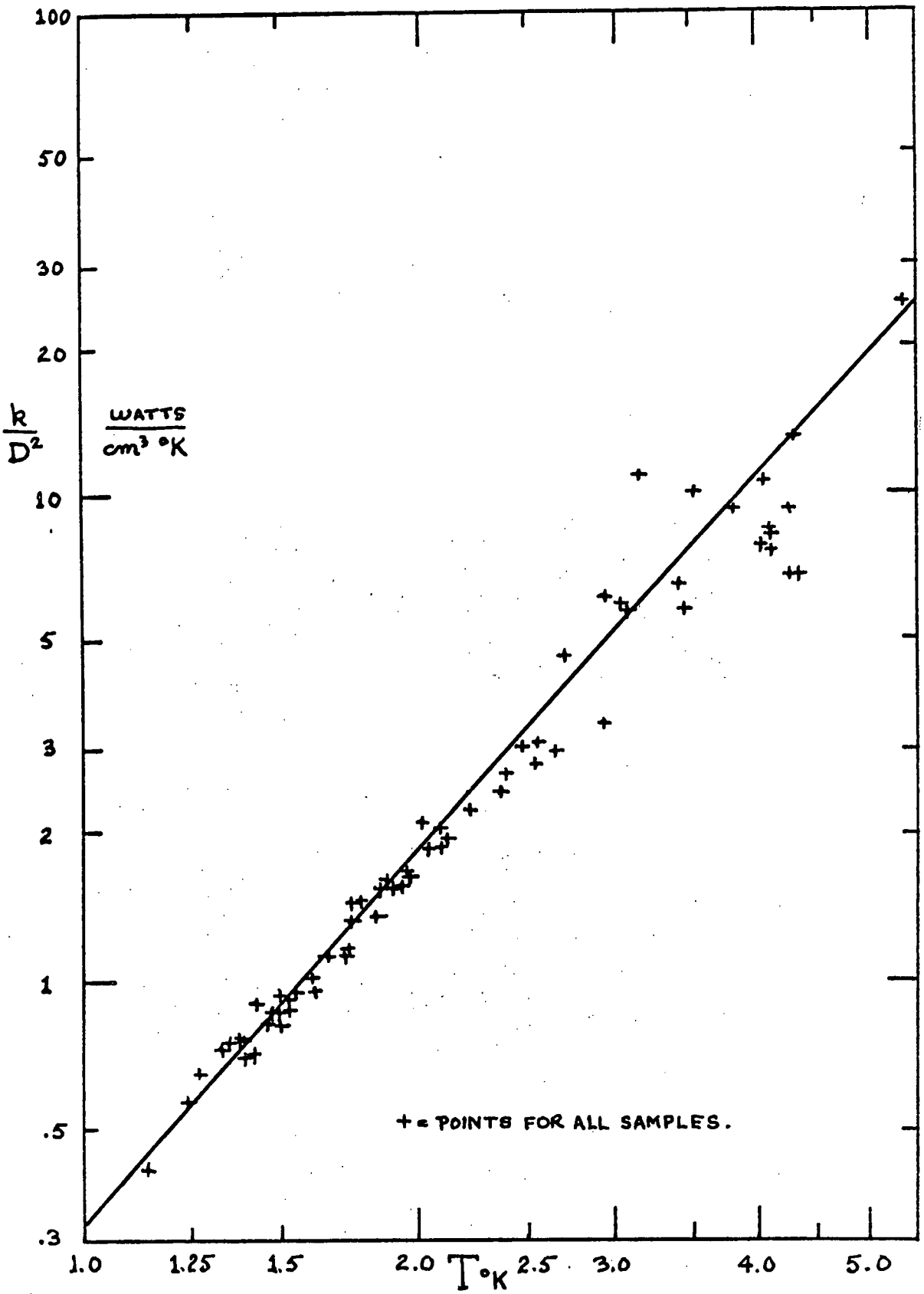

SIZE DEPENDENCE - B.

FIGURE 11

a dependence on T^3. However, it may be seen from Figures 9 or 10 that k is very strongly size dependent, or at least sample dependent. We thus conclude that k is affected by sample size, or internal sample structure, or both.

(b) Internal Structure Dependence. If the conductivity is being determined by internal sample structure there are three major phonon scattering mechanisms which should be considered, (i) point defect scattering, (ii) line dislocation scattering, and (iii) grain boundary scattering.

Both Cs and I have only one naturally occurring isotope. CsI is therefore isotopically pure. The CsI used was also of "optical purity" with regard to chemical impurities. We may therefore rule out point defect scattering as a dominant mechanism. Point defect scattering would introduce a temperature dependence of T^{-1} in the thermal conductivity.

Line dislocation scattering can be shown (Klemens, 1958) to introduce a temperature dependence of T^2 in the thermal conductivity. The thermal resistance due to line dislocations is

$$\frac{1}{k_L} \cong \frac{1}{T^2} \frac{h^2 v \gamma^2}{60K \times 7.05} N_L b^2 \qquad (7),$$

where N_L is the average number of dislocation lines per unit area, b is the average Burger's vector of the dislocations, γ is the Gruneisen parameter for the material, and v is the velocity of sound in the material.

It may also be shown (Klemens, 1956) that grain boundary scattering would introduce a temperature dependence of T^3 in the thermal conductivity. The thermal resistance due to grain boundaries was shown to be approximately

$$\frac{1}{k_G} \cong \frac{3}{C_v v L} \qquad (8),$$

where C_v is the specific heat, v is the average velocity of sound and L is either the sample size, or $L = l\alpha^2$ where l is the average distance between grain boundaries and α is the average angle of tilt.

Let us suppose that the thermal conductivity of our samples is governed by some combination of line and plane dislocation scattering. We may then say that the thermal resistance 1/k is roughly given by

$$\frac{1}{k} = \frac{G}{T^2} + \frac{H}{T^3} \qquad (9),$$

(where G and H are constants for a given sample), i.e. that the thermal resistance is the sum of the thermal resistance due to line dislocation scattering, and the thermal resistance due to grain boundary scattering.

The measured conductivities in this experiment were shown to depend on $T^{2.58}$, whence the measured thermal resistance

is given by

$$\frac{1}{k} = \frac{A^{-1}}{T^{2.58}} \qquad \text{---------- (10).}$$

Suppose we equate these expressions,

$$\frac{A^{-1}}{T^{2.58}} = \frac{G}{T^2} + \frac{H}{T^3} \qquad \text{---------- (11)}$$

and solve for G and H by substitution of two temperatures, say 1.5°K and 4.0°K, using one of the measured values of A^{-1}. Doing this gives values of G and H and a ratio of G:H of about 1:3. Subsequent evaluation of (9) and comparison with (10) shows that if k were given by equation (9) instead of equation (10), it would differ from (10) by no more than 5% over the measured temperature range. The data does not permit us to distinguish between the two possibilities (9) and (10) and we may therefore conclude that a behaviour of the form indicated by (9) is a possibility in the light of the present experiment.

As a further check on the possibility of line and plane dislocation scattering, one may use the calculated magnitudes of G and H to estimate the defect concentrations. A number of numerical assumptions must be made, but by choosing an individual case one may estimate the grain boundary separation-

-tilt angle product, and the line dislocation density. In the case of sample #3, for instance, if one assumes large crystallites (of the order of 1/10 of the sample diameter), one obtains from H and (8) an average tilt angle of about 15°, and from G and (7) a dislocation line density of about $5 \times 10^8/cm^2$ (taking the average Burger's vector to be a few lattice spacings). The dislocation density of $5 \times 10^8/cm^2$ is rather high, but experiments on the effect of dislocations in LiF have shown (Sproull et al, 1959) that Klemens' equation does seem to produce a value much too high. Sproull noted a discrepancy of about 5×10^3. If we reduce N_L by this factor we obtain a value of $N_L \sim 10^5/cm^2$, a dislocation density typical of a slightly strained alkali halide crystal.

It should also be noted here that the dislocation density estimated for sample #3 is higher than that estimated for sample number one. This would be expected since sample #3 was ground down from sample #1, the grinding process being quite likely to introduce strains and consequent dislocations.

The validity of the above interpretation could be checked by annealing one of the samples and remeasuring its conductivity. If dislocation scattering is a dominant mechanism, the conductivity of an annealed sample would be expected to be considerably higher than that observed previous to the annealing.

It should be noted that if dislocation scattering is responsible for governing the thermal conductivity of these CsI samples, then any functional relationship between sample diameter and thermal conductivity is strictly coincidental. The apparent proportionality of k to the square of the sample diameter for our specimens is rather striking, and the author would be surprised to find that it is coincidental.

Coincidences, however, do tend to be surprising. We intend to investigate the thermal conductivity of samples of other sizes, and to investigate the effect of annealing the samples to resolve the question of the existence of size dependence and/or internal structure dependence in this material.

BIBLIOGRAPHY

Berman, R., Simon, and Ziman: Proc. Roy. Soc. A220, 171 (1953)

Berman, R.: Rev. Sci. Inst. 25, 94 (1954)

Berman, R., Foster, and Ziman: Proc. Roy. Soc. A231, 130 (1955)

Berman, R.: Cryogenics 5, 297 (1965)

Betts, D.D., Bhatia, and Wyman: Phys. Rev. 104, 37 (1956)

Callaway, J.: Phys. Rev. 113, 1046 (1959)

Callaway, J.: Phys. Rev. 122, 787 (1961)

Carruthers, P.: Rev. Mod. Phys. 33, 92 (1961)

Casimir, H.B.G.: Physica 5, 495 (1938)

Clement, J.R., and Quinnel: Rev. Sci. Inst. 23, 213 (1952)

deHaas, W.J., and Biermasz: Physica 5, 619 (1938)

Guyer, R.A., and Krumhansl: Phys. Rev. 148, No. 2, 778 (1966)

Houston, W.V.: Rev. Mod. Phys. 20, 161 (1948)

James, B.W., and Yates: Cryogenics 5, 68 (1965)

Johnson, R.C., and Little: Phys. Rev. 130, 596 (1963)

Klemens, P.G.: in Handbuch der Physik, (Springer-Verlag, Berlin 1956). Volume 14

Klemens, P.G.: in Solid State Physics, (Academic Press, Inc., New York 1958). Volume 7

Makinson, R.E.B.: Proc. Cambridge Phil. Soc. 34, 474 (1938)

Peierls, R.E.: Ann. Physik 3, 1055 (1929)

Sproull, R.L., Moss, and Weinstock: J. Appl. Phys 30, 334 (1959)

Taylor, A.R., Gardner, and Smith: Bureau of Mines Rep. No. 6157. (U.S. Department of the Interior, 1963)

Thatcher, P.D.: PhD. Thesis, Cornell University, (1965)

Vallin, J., Beckman, and Salama: J. Appl. Phys. 35, 1222 (1964)

van Dijk, H., Durieux, Clement, Logan, and Brickwedde: Journal of Research of the National Bureau of Standards - A. Physics and Chemistry 64A, No. 1 (1960)

Walker, E.J.: Rev. Sci. Inst. 30, 834 (1959)

Ziman, J.M.: Can. J. Phys. 34, 1256 (1956)

APPENDIX 1

Density, Volumetric Expansion and Relative Density of Butyl Phthalate.

(a) In order to obtain an accurate correspondence between the oil (butyl phthalate) manometer and the mercury manometer, it was desired to know the ratio of the density of butyl phthalate to mercury as a function of temperature in the room temperature range. Butyl phthalate ($C_{16}H_{22}O_6$) is also called dibutyl phthalate, n-butyl phthalate and phthalic acid, dibutyl ester.

We were unable to find measurements of the density of this material as a function of temperature. Furthermore, the density quoted in the Handbook of Chemistry and Physics (1964-1965) disagreed with that on the bottle label. We therefore decided to perform the experiment ourselves.

(b) A density bottle with attached capillary was used to determine the volume of a sample of oil. The bottle was weighed, then accurately calibrated using double distilled water. The oil used was 21.800 $\pm$ .001 gm of butyl phthalate supplied by the Fisher Scientific Company, Lot number 753885. Immediately prior to placing it in the density bottle, the oil was thoroughly outgassed by pumping on it with a rotary

vacuum pump for a period of 24 hours.

The absolute density of the oil was established by direct measurement of mass and volume at two temperatures. The density over the range 17 - 24°C was measured by observing the meniscus level of the oil in the capillary via a cathetometer, and subsequently computing the volume of the oil. The experiment was performed with the entire density bottle immersed in a large water bath. Temperatures were measured at various points in the water bath and agreed to within .1°C.

In computing the volume, density and expansion coefficient of the butyl phthalate, the thermal expansion of the Pyrex density bottle had to be considered. The value of the volumetric expansion coefficient for Pyrex was taken to be (Handbook of Chemistry and Physics, 1964)

$$\beta_g = (9.3 \pm .3) \times 10^{-6}/°C \quad \text{---------- A(1).}$$

The direct measurement of the density of butyl phthalate yielded the results

$$\rho_{oil}\ (22.0°C) = 1.0456 \pm .005\ gm/cm^3 \quad \text{---------- ,}$$

and $$\rho_{oil}(20.7°C) = 1.0467 \pm .005\ gm/cm^3 \quad \text{---------- A(2).}$$

Measurement of the meniscus level in the capillary, and subsequent calculations yielded the values of $\bar{\beta}_{oil}$, $\rho_{oil}(T)$, $\rho_{Hg}(0)/\rho_{oil}(T)$ and $\rho_{Hg}(T)/\rho_{oil}(T)$ shown in Table A:1. The

TABLE A: I

Expansion Properties of Butyl Phthalate ($C_{16}H_{22}O_4$).

$$\overline{\beta}_{oil} = \frac{\text{Volume } (T°C) - \text{Volume } (0\,°C)}{[\text{Volume } (0\,°C) \times T°C\ ]}$$

$$= (.85 \pm .01) \times 10^{-3}/°C \text{ at } 22°C.$$

T°C	$\rho_{oil}(T)$ gm/cm^3	$\rho_{Hg}(0)/\rho_{oil}(T)$	$\rho_{Hg}(T)/\rho_{oil}(T)$
0 ± .1	1.0652 ± .0007	12.762 ± .007	12.762 ± .007
5	1.0606 "	12.818 "	12.807 "
10	1.0562 "	12.871 "	12.848 "
15	1.0517 "	12.926 "	12.891 "
16	1.0509 "	12.936 "	12.899 "
17	1.0500 "	12.947 "	12.907 "
18	1.0491 "	12.958 "	12.916 "
19	1.0482 "	12.969 "	12.925 "
20	1.0473 "	12.981 "	12.934 "
21	1.0465 "	12.991 "	12.941 "
22	1.0456 ± .0005	13.002 "	12.950 "
23	1.0447 "	13.013 "	12.959 "
24	1.0439 "	13.023 "	12.966 "
25	1.0430 "	13.034 "	12.975 "
26	1.0421 "	13.045 "	12.984 "
27	1.0413 "	13.055 "	12.992 "
28	1.0404 "	13.067 "	13.000 "
29	1.0395 "	13.078 "	13.009 "
30	1.0387 "	13.088 "	13.017 "

mercury density values used in the oil to mercury density ratio calculation were taken from the 1954 Smithsonian Physical Tables (The Smithsonian Institution, 1954).

$\overline{\beta}_{oil}$ was found to be essentially constant over the measured temperature range.